MODELING AND CONTROL OF QUADROTOR UAV WITH TILTING ROTORS

BY

MAHMOUD ELFEKY

A Thesis Presented to the

DEANSHIP OF GRADUATE STUDIES

KING FAHD UNIVERSITY OF PETROLEUM & MINERALS

DHAHRAN, SAUDI ARABIA

In Partial Fulfillment of the
Requirements for the Degree of

MASTER OF SCIENCE

In

SYSTEMS AND CONTROL ENGINEERING

APRIL 2015

KING FAHD UNIVERSITY OF PETROLEUM & MINERALS
DHAHRAN 31261, SAUDI ARABIA

DEANSHIP OF GRADUATE STUDIES

This thesis, written by **MAHMOUD ELFEKY** under the direction of his thesis adviser and approved by his thesis committee, has been presented to and accepted by the Dean of Graduate Studies, in partial fulfillment of the requirements for the degree of **MASTER OF SCIENCE IN SYSTEMS AND CONTROL ENGINEERING**.

Thesis Committee

M. Elsh.

Dr. Moustafa Elshafei (Adviser)

Dr. Abdulwahid Alsaif (Member)

Dr. Sami Elferik (Member)

عادل

Dr. Adel Fadhel Ahmed
Department Chairman

Dr. Salam A. Zummo
Dean of Graduate Studies

30/4/15

Date

Dedication

To my parents for their endless sincerity and support. To the memory of my beloved sister, Asmaa, whose smile and words will always linger on; and to my siblings for being the source of happiness at all times.

ACKNOWLEDGMENTS

In the name of Allah, The most gracious, the most merciful. My appreciation to King Fahd University of Petroleum and Minerals for providing a great environment for research and innovation. I would like to particularly thank my advisor Dr.Moustafa Elshafei and committee members Dr.Sami Elferik and Dr.Abdul-Wahid A. Saif for their guidance, patience and support. Without them this work would have not been possible.

TABLE OF CONTENTS

LIST OF TABLES

LIST OF FIGURES

THESIS ABSTRACT

NAME:	Mahmoud Elfeky
TITLE OF STUDY:	Modeling and Control of Quadrotor UAV with Tilting Rotors
MAJOR FIELD:	Systems and Control Engineering
DATE OF DEGREE:	April 2015

Quadrotors have recently been drawing greater attention to the point that they have become one of the most popular unmanned aerial vehicles types. Their applications vary from entertainment to transportation, commercial and even military applications.

In this Thesis, a novel quadrotor design is proposed. The design decouples all motions by allowing each rotor to tilt in two directions about its fixed frames. This modification improves the stability and safety of the quadrotor and gives it more manoeuvrability and robustness. The model is presented along with a proposed operator control panel for manned application. Several flight scenarios are also simulated under a simple PID controller to illustrate the superiority over conventional quadrotor designs as initial tests.

In addition, a Feedback linearization controller is developed to control the states of the quadrotor. This controller is implemented in a way that not only decouples the motions, but also decouples the system model itself into two completely separate systems with separate controllers. Stability of the controller is improved using Lyaponov theorem under different conditions.

Furthermore, several optimization techniques are tested to choose among the combinations of inputs. The objective of optimization is to minimize energy consumption during flights, which is a critical issue in unmanned aerial vehicles. The results of the controller are illustrated by simulations and virtual reality model. A comparison between optimization techniques based on convergence time is also presented

ملخص الرسالة

الإسم: محمود الفقي

عنوان البحث: النمذجة الرياضية والتحكم في الطائرة الرباعية ذات المحركات القابلة للدوران

التخصص: هندسة النظم والتحكم

تاريخ التسليم: أبريل 2015

تعتبر الطائرة رباعية المحركات من مواضيع البحث التي جذبت اهتمام الباحثين الى درجة أنها أصبحت واحدة من أكثر أنواع الطائرات الذاتية جاذبية. حيث تتنوع تطبيقات هذه الطائرة بين الألعاب ووسائل المواصلات والأغراض التجارية وصولا إلى المراقبة والأغراض العسكرية. هذه الرسالة البحثية تقدم تصميماً جديداً من الطائرات رباعية المحركات حيث يتم السماح لكل محرك بالدوران حول محورين ثابتين. تسمح هذه الإضافة بفصل جميع الحركات الممكنة للطائرة كما تحسَّن الثبات والأمان للطائرة بشكل واضح وتعطيها رشاقة وقابلية للحركة بحرية أكبر. تعرض هذه الرسالة البحثية نموذجاً رياضياً للطائرة المقدمة كما تعرض نظاما للتشغيل اليدوي عن طريق طيار في حال تم تصميمها لهذا الغرض. تم تصميم برنامج لمحاكاة النموذج وتجربة عدد من المناورات من خلاله لأثبات أفضلية التصميم الجديد وقد تم استخدام نظام التحكم PID خلال هذه المناورات الابتدائية.

الخطوة التالية هي تصميم نظام تحكم متكامل باستخدام تقنية تحويل النموذج الغير خطي الى خطي عن طريق المداخل والمعروفة بـ feedback linearization حيث تم تجزئة نظام الطائرة الى نظامين منفصلين تماما يمكن التحكم في كل منهما دون ارتباط بالآخر. تمت دراسة ثبات نظام التحكم بواسطة نظرية ليابونوف وبافتراضات متنوعة. تم أيضا اضافة نظام مفاضلة لاختيار أقل الحلول المتاحة من المداخل استهلاكا للطاقة, حيث تعتبر الطاقة أحد أهم المواضيع البحثية في الطائرات ذاتية الطيران. كما تمت مقارنة مجموعة من تقنيات المفاضلة من حيث الوقت اللازم للوصول الى نتيجة وأفضلية النتيجة ذاتها. في النهاية استحدث برنامج لمحاكاة نظام التحكم مع المفاضلة وتمت اختبار النظامين عن طريق مجموعة من المناورات المعقدة حيث أظهرت المحاكاة نتائج مبشرة للغاية سواء من جهة نظام التحكم أو من جهة نظام المفاضلة.

CHAPTER 1

INTRODUCTION

1.1 Overview

A quadrotor is a flying robot with four propellers fixed at the ends of two crossing axes. The four propellers create thrust that allows the quadrotor to hover and fly in different directions. A typical flying robot has six degrees of freedom: 3 translational and 3 rotational. However, quadrotor has only four rotating propellers which limits it's capability in moving freely as will be discussed later.

During the past decade, UAV quadrotor has drawn more and more research attention. Its simple design makes it very attractive for tasks such as surveillance, data collection, search and rescue missions and even carrying small objects. However, very little research, if any, targeted quadrotor as a manned aerial vehicle (QARV).

Quadrotor Air Vehicles (QARV) may be employed in a wide range of commercial and military applications. Such applications may include: heavy transporta-

tion, construction of bridges and buildings, assembly of large pieces in factories, and rescue operations after natural disasters where roads and bridges are no longer usable. For military applications, QRAV may perform vertical takeoff and landing (VTOL) and can be used in manned operations for effective transport and for military deployment operations in hostile environments where VTOL is a requirement. Additionally, QRAV can have manoeuvrability that may be superior to helicopters, such as the APACHE helicopter.

1.2 Motivation

Conventional quadrotor is typically underactuated. It is composed of four fixed rotors which provide four input variables and has six degrees of freedom (DOF), 3 position and 3 orientations. The underactuated nature of typical quadrotors forces two translational motions to be coupled with two rotational orientations, i.e. the x and y translation motions are coupled with the two rotational angles pitch and roll respectively. This coupling reduces the manoeuvrability and agility and severely limits tracking capabilities. For example, to move forward or sideways, roll or pitch angles is compromised and the UAV has to tilt. The UAV cannot go through tight openings and can't hover while having a tilted orientation. While these limitations are not of big impact on ordinary missions, critical missions demand much higher manoeuvrability.

In addition to limitations in maneuverability, fault tolerance capabilities in conventional quadrotor is quiet low. Loss of any of the propellers would severely

impact the behavior of the quad. However, there is a great potential for physical improvement to overcome these issues.

The way feedback linearization is developed here decouples the model of the system into two subsystems of forces/positions and moments/orientations. The two resulted systems are can be controlled completely separately and independently which has not been done before in quadrotors.

1.3 Objectives

The objective of this work is to introduce a novel quadrotor design with physical improvements to overcome limitations present in conventional quadrotor. The proposed design allows each rotor to tilt freely on a hemisphere. The objectives include

- Modeling of the novel system
- Designing a controller to exploit the physical advantages.
- Designing an algorithm to optimize the inputs of the system

1.4 Outline

This thesis is organized as follows: Chapter 2 presents literature review for the topic. Chapter 3 presents the modeling of the new system. In chapter 4, a feedback linearization controller is designed for the quadrotor. Finally, chapter 5 presents concluding remarks for this work.

CHAPTER 2

LITERATURE REVIEW

2.1 VTOL and Quadrotor Design and Control

Vertical take off and landing vehicles (VTOL) are becoming more and more popular. Their ability to take off and land vertically means that they don't need a runway which is a very critical in almost all applications. Hence, research targeting VTOL design and control have been drawing more attention.

In [1], one of the first tilt-wing VTOL aircrafts was designed and tested to explore the feasibility of transition from hover to forward flight. Various Problems that are related to the performance and control characteristics were discussed. However, at the time, the paper concluded that it was very early to determine control requirement due to lack of flights data. [2] presents a general control approach of autonomously flying VTOL robots that takes advantage of the similarity in motion description in different VTOL robots. This control scheme is based on linearization using inversion of the model blocks. It was shown that this general

scheme with inversion of the model blocks works even if the non-linear parameters are unknown.

Specifically, quadrotors are one type of VTOL has been under the focus of extensive research due to their simple design and high agility. This research essentially covered areas such as modeling and control of the system. Conventional quadrotor modeling and control were extensively covered in the literature. In [3], the author describes an efficient and robust quadrotor for both indoor and outdoor. The paper presented an improvement to overcome uncertainty in position control and instability during fast maneuverer caused by low frequency in the control.

[4] presents development and accurate modeling for a quadrotor UAV. The developed system was equipped with necessary devices and sensors. Rigorous dynamic model and robust flight control is developed. The controller presented is a disturbance observer based controller.

In [5], a fully autonomous quadrotor was presented for indoor applications. While navigation of outdoors quadrotor depends mainly on Global Positioning System (GPS), indoor quadrotors can not rely on that type of systems. Hence, the paper presented a navigation systems to enable small quadrotors to operate autonomously in closed environments. The approach was an extension and adaptation of techniques successfully implemented in ground robots.

[6] presented a customized design for control system validation. The paper presented an L1 mathematical modeling that defines the 6 degrees of freedom. The model is described in details and the complexity of L1 was claimed to aim

at describing the key features of the flight. In [7], a relatively large quadrotor was presented. The UAV was designed to weigh 4 kg and have a payload of 1 kg. This improvement aimed to exploit the advantages of quadrotor maneuverability in more applications where carrying objects is desirable.

A new quaternion-based feedback control scheme for attitude stabilization of quadrotor is proposed in [8]. The controller has the structure of feedback PD^2 controller to compensate for coriolis and gyroscopic torques. More on quadrotor design and control can be found in [9], [10], [11], [12] and [13]

2.2 Tilting Mechanism

Many breakthroughs emerged by researchers trying to overcome the actuation difficulties in UAV's. Tilt wing mechanism was proposed in [14] and tilt rotor actuation in [15], [16]. In [14], a hybrid system of an aerial vehicle was presented that has a tilt-wing mechanism. The vehicle is capable of vertical takeoff/landing like a helicopter as well as flying horizontally like an airplane. This is done by mounting four rotors on four rotating wings.

[15] presented a mini tilt-rotor UAV with two rotors. Modeling of the system was discussed and the dynamics of the 6 DOF's were split into three subdynamics to simplify the control task. The system was equipped with extra mass to introduce a pendular damped effect.

In [16], a proposed system with two rotors was presented. The two rotors are allowed to tilt laterally and longitudinally to control the thrust direction. A

prototype was implemented and tested and showed promising results in terms of hovering and pitch stability.

In order to maintain a zero net yaw moment, [17] proposed slightly slanted two opposite propellers with a small angle. It was shown that the four main movements : roll, pitch, yaw and heave can be completely separated using this design.

In [18], a novel quadrotor design was presented. The four rotors were allowed to rotate about their axes w.r.t the main rotor body. This adds four extra inputs to have a total of eight inputs to the quadrotor. The design provides full actuation to the quadrotor position/orientation with two extra inputs.

2.3 Fault Tolerance

Fault tolerance has been one of the main concerns in the area of flying vehicles. [19] and [20] discuss fault tolerance in system design. Many researchers targeted fault tolerance in quadrotors from the control point of view. In [21], the case of a quadrotor with one faulty rotor is investigated. A double control loop architecture was proposed to assure trajectory tracking on translational motions as well as roll and pitch rotations. The method was claimed to achieve the desired control with acceptable behavior. However, Yaw movement was compromised and the quadrotor keeps rotating around its z-axis.

A sliding mode approach to control quadrotor UAV in case of external disturbance and actuator fault was used in [22]. The method was proven to distinguish

between disturbances and faults and the simulation verified the effectiveness of the method. However, the same challenge of yaw angle occurs. Yaw motion tends to go out of control.

Considerable research targeting fault tolerance suggest the use of actuator redundancy. In [23], an integral sliding control was used to handle total actuator failures directly without changing the baseline controller. The controller takes advantage of the present redundancy of actuators without the need for fault detection and isolation. Similarly, [24] presented a fault tolerant controller that uses Linear Parameter Varying (LPV) sliding mode technique to exploit redundancy without the need for fault detection and isolation.

2.4 Feedback Linearization

Feedback linearization have been one of the most common control techniques to overcome the nonlinearities in conventional quadrotors dynamics. The theory of linearizing a non-linear system through feedback is covered thoroughly in the literature [25], [26], [27], [28], [29] and [30].

In [31], a nonlinear control of micro-quadrotor using feedback linearization was discussed. The control system was developed by decomposing the dynamics into nested loops. Both the inner loop position control and the outer loop velocity control showed effectiveness with feedback linearization technique.

[32] shows a feedback linearization technique with a dynamic extension that lead to a fourteenth dimensional controller for the twelve state system. The con-

troller was able to completely linearize the highly non-linear dynamics.

In [33], a feedback linearization-based controller with a high order sliding mode observer was introduced to control quadrotor. The controllers were applied in parallel where the high order sliding mode observer worked as an observer and estimator for the effect of external disturbances. Although the technique linearizes the dynamics of the UAV, the disturbances effects remain nonlinear which makes the linearization non-robust. The sliding mode technique contributed in avoiding the chattering around desired trajectories.

A comparison between feedback linearization and adaptive sliding mode control is presented in [34]. Although feedback linearization is simple to implement, performance can be compromised in the presence of model uncertainty. In addition, the controller was showed to be sensitive to noise due to the presence of high order differentiation. In contrast, a proposed adaptive sliding mode technique showed robustness to uncertainty and sensor noises.

2.5 Optimization for Control

Interior-Point optimization was discussed in details in [35] and in [36] with applications in process engineering. Genetic algorithms was generally covered in [37], [38], [39] and [40].

The mating between optimization and control theory have produced more theories and techniques. Optimal Control and Model Predictive Control are two of the most famous techniques were optimization is used in control theory. [41]

discusses some aspects of the relation between optimization and control theory.

A robust constrained Model Predictive Control is implemented in [42] using linear matrix inequalities. Thee aim of using this technique is to overcome the primary disadvantage in conventional MPC which is the inability to explicitly deal with model uncertainty. The proposed technique is tested with uncertainties expressed in both time and frequency domain and was able to stabilize the set of uncertain plants.

[43] presents a modified genetic algorithms for optimal control problems. The technique was compared with General Algebraic Modeling System (GAMS) optimization and showed superiority. In [44], a model based optimal control technique is used with genetic algorithm. The genetic algorithm is implemented to solve the online optimization problem. The results show that the strategy used was capable of optimizing the overall performance of the system.

CHAPTER 3

SYSTEM MODELING AND INITIAL TESTS

3.1 Introduction

In this chapter, a novel quadrotor design is introduced that has advantages for both manned and unmanned applications. Each rotor is allowed to tilt around two axes w.r.t fixed body frame. The total number of inputs is increased to twelve. Although six inputs are enough to have a fully actuated system, twelve inputs may be required to impose arbitrary trajectories to more output independently. With this design, each of the twelve states (outputs) (6 positions/orientations - 6 transitional/rotational speeds) can be controlled independently and freely. In addition, the system can perform all the desired control objectives with half of its actuators faulty. More advantages and distinguished capabilities for critical missions are discussed later in this chapter.

This chapter is organized as follows: section 1 presents the dynamic model of quadrotor with two DOF's tilting propellers. Section 2 discusses the advantages of this design over conventional designs for manned operations and proves some of these advantages with simulation. Finally, the chapter is concluded in section 3.

3.2 System Model

3.2.1 Frames and Rotation Matrices

The quadrotor can be considered as five rigid bodies connected together and are in relative motion around themselves. Those five bodies are the quadrotor body itself $\boldsymbol{B}$, and four propellers $\boldsymbol{P}_i$ attached to the body.

Let $\mathcal{F}_E : \{O_E; \quad X_E, \quad Y_E, \quad Z_E\}$be a world inertial fram and $\mathcal{F}_B : \{O_B; \quad X_B, \quad Y_B, \quad Z_B\}$ be the quadrotor body frame attached to its center of gravity. In addition, the rotors-fixed frames are taken to be parallel to each other and parallel to the quadrotor body frame and are given by $\mathcal{F}_{P_i} : \{O_{P_i}; \quad X_{P_i}, \quad Y_{P_i}, \quad Z_{P_i}\}$, $i = 1, ..., 4$.

The orientation of each of the rotors is controlled by two rotations with respect to the rotor-fixed frame; α_i, a rotation about Y_{P_i}, and β_i , about Z_{P_i}. This rotation creates a second rotating frame for the rotors, $\mathcal{F}_{\overline{P}_i} : \{O_{\overline{P}_i}; \quad X_{\overline{P}_i}, \quad Y_{\overline{P}_i}, \quad Z_{\overline{P}_i}\}$, $i = 1, ..., 4$.

When the rotors are aligned along Z_{P_i}, rotor 1 and rotor 2 are assumed to

rotate counter-clock-wise CCW, while rotor 3 and rotor 4 rotate clock-wise CW. The forward direction is taken arbitrary to be along X_B

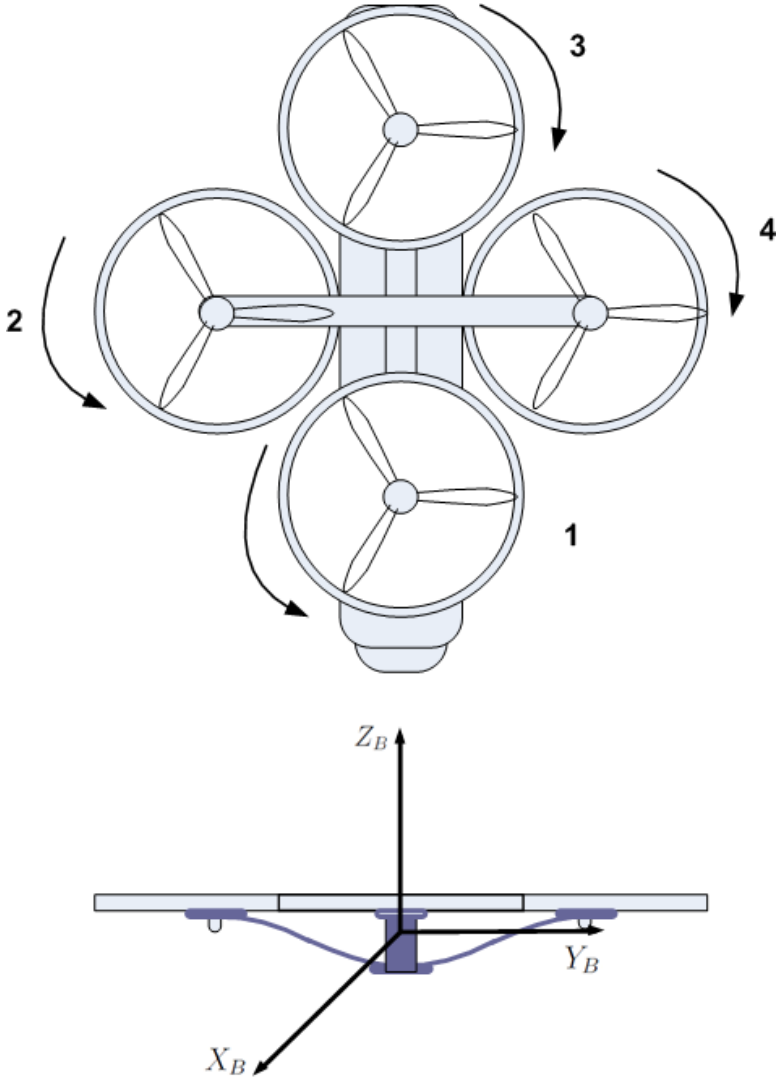

Figure 3.1: Quadrotor with each rotor tilting about two axes

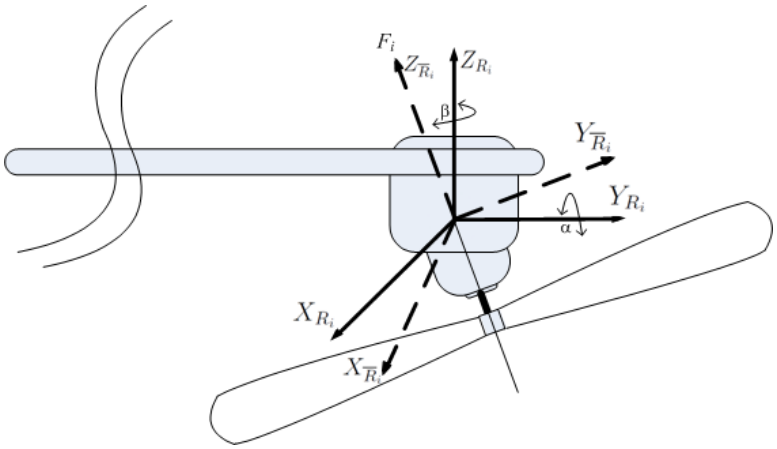

Figure 3.2: Tilt angles of the rotor w.r.t fixed body frames

Let $R^{P_i}_{\overline{P}_i}$ be the rotational matrix from the rotors-rotating frame $O_{\overline{P}_i}$ to the rotors-fixed frame O_{P_i}. Since the rotors-fixed frames O_{P_i} are parallel to the body-fixed frame O_B at the center of gravity, then

$$R^{P_i}_{\overline{P}_i} = R^{B}_{\overline{P}_i} = \begin{bmatrix} 0 & 0 & C\beta_i S\alpha_i \\ 0 & 0 & S\beta_i S\alpha_i \\ 0 & 0 & C\alpha_i \end{bmatrix} \tag{3.1}$$

where $C(.)$ and $S(.)$ denote $cos(.)$ and $sin(.)$ respectively.

A full rotation of the quadrotor body with respect to the inertial frame can be described by three consecutive rotations about the three body axes, roll rotation Φ about the body x-axis, pitch rotation Θ about the body y-axis and yaw rotation Ψ about the body z-axis. Then R^E_B is the body transformation matrix with respect to the earth inertial frame, and is given by

$$
\begin{aligned}
R_B^E &= R_\Psi \bullet R_\Theta \bullet R_\Phi \\
&= \begin{bmatrix} C\Psi & -S\Psi & 0 \\ S\Psi & C\Psi & 0 \\ 0 & 0 & 1 \end{bmatrix} \begin{bmatrix} C\Theta & 0 & S\Theta \\ 0 & 1 & 0 \\ -S\Theta & 0 & C\Theta \end{bmatrix} \begin{bmatrix} 1 & 0 & 0 \\ 0 & C\Phi & -S\phi \\ 0 & S\Phi & C\phi \end{bmatrix} \\
&= \begin{bmatrix} C\Psi C\Theta & -S\Psi C\Phi + C\Psi S\Theta S\Phi & S\Psi s\Phi + C\Psi S\Theta C\Phi \\ S\Psi C\Theta & C\Psi C\Phi + s\Psi S\Theta S\Phi & -C\Psi S\Phi + S\Psi S\Theta C\Phi \\ -S\Theta & C\Theta S\Phi & C\Theta C\Phi \end{bmatrix}
\end{aligned} \tag{3.2}
$$

The relationship between the body-fixed angular velocity vector $[p \quad q \quad r]^T$ and Euler-Angles rates $[\dot{\Phi} \quad \dot{\Theta} \quad \dot{\Psi}]^T$ is given by

$$
\begin{bmatrix} p \\ q \\ r \end{bmatrix} = \begin{bmatrix} 1 & 0 & -S\Theta \\ 0 & C\Phi & S\Phi C\Theta \\ 0 & -S\Phi & C\Phi C\Theta \end{bmatrix} \begin{bmatrix} \dot{\Phi} \\ \dot{\Theta} \\ \dot{\Psi} \end{bmatrix} \tag{3.3}
$$

3.2.2 Quadrotor Dynamics

Assume that the rotational speed of the rotor i is given by w_i. Then we can say that the lifting thrust is given $b\omega_i^2$ and the drag moment is given by $d\omega_i^2$, where b and d are the thrust and drag moment constants respectively.

The thrust components of the i^{th} rotor at the body C.G. are then given by

$$F_i = \begin{bmatrix} 0 & 0 & C\beta_i S\alpha_i \\ 0 & 0 & S\beta_i S\alpha_i \\ 0 & 0 & C\alpha_i \end{bmatrix} \begin{bmatrix} 0 \\ 0 \\ b\omega_i^2 \end{bmatrix} \tag{3.4}$$

Similarly, the moments of a titled rotor consist of two parts, the drag moment, and the moments generated by the thrust components. These two components can be expressed as

$$M_i = \begin{bmatrix} 0 & 0 & C\beta_i S\alpha_i \\ 0 & 0 & S\beta_i S\alpha_i \\ 0 & 0 & C\alpha_i \end{bmatrix} \begin{bmatrix} 0 \\ 0 \\ d\omega_i^2 \delta(i) \end{bmatrix} + r_i \times F_i \tag{3.5}$$

where $\delta = [1, 1, -1, -1]$ and r_i is the vector from center of gravity to the reference point of the rotors, i.e.

$$r_1 = [l, 0, -h] \qquad r_2 = [0, l, -h]$$

$$r_3 = [-l, 0, -h] \qquad r_4 = [0, -l, -h]$$

h and l represent the vertical and horizontal displacements from the center of gravity to the rotors respectively.

The quadrotor position vector η and body angular velocities vector Ω are given by

$$\eta = [x \quad y \quad z]^T$$

$$\Omega = [p \quad q \quad r]^T$$

The summation of forces acting on the quadrotor body is then given by the dynamic equation:

$$m\ddot{\eta} = mg_z - K\dot{\eta} + R_B^E \sum_{i=1}^{4} F_i \tag{3.6}$$

where m is the mass of the quadrotor, and

$$g_z = [0 \quad 0 \quad -g]^T$$

K is the matrix of drag constants, and is given by

$$K = \begin{bmatrix} K_1 & 0 & 0 \\ 0 & K_2 & 0 \\ 0 & 0 & K_3 \end{bmatrix}$$

The rotation dynamic equation is then given by:

$$I\dot{\Omega} = -(\Omega \times I\Omega) - M_G + \sum_{i=1}^{4} M_i \tag{3.7}$$

where I is the inertia matrix of the quadrotor, and is given by

$$I = \begin{bmatrix} I_x & 0 & 0 \\ 0 & I_y & 0 \\ 0 & 0 & I_z \end{bmatrix}$$

M_G is the gyroscopic forces, and is give by

$$M_G = \sum_{i=1}^{4} I_R(\Omega \times \overline{\omega}_i)\delta(i) \tag{3.8}$$

I_R is the rotor moment of inertia. And

$$\overline{\omega}_i = \begin{bmatrix} 0 & 0 & C\beta_i S\alpha_i \\ 0 & 0 & S\beta_i S\alpha_i \\ 0 & 0 & C\alpha_i \end{bmatrix} \begin{bmatrix} 0 \\ 0 \\ \omega_i \end{bmatrix} \tag{3.9}$$

The equations of motion can be put in the standard form

$$\dot{X} = f(X, U)$$

where

$$X = [\dot{\eta} \quad \Omega]^T$$

$$U = [\omega_1 \quad \alpha_1 \quad \beta_1 \quad \omega_2 \quad \alpha_2 \quad \beta_2 \quad \omega_3 \quad \alpha_3 \quad \beta_3 \quad \omega_4 \quad \alpha_4 \quad \beta_4]^T$$

$$\begin{bmatrix} \ddot{\eta} \\ \dot{\Omega} \end{bmatrix} = \begin{bmatrix} g_z - \frac{K}{m}\dot{\eta} + \frac{R_B^E}{m}\sum_{i=1}^{4} F_i \\ -(I^{-1}\Omega \times \Omega) - I^{-1}M_G + I^{-1}\sum_{i=1}^{4} M_i \end{bmatrix} \tag{3.10}$$

where F_i and M_i are related to the elements of the input vector U through equations (3.4) and (3.5) respectively.

3.3 PILOT CONTROL COMMANDS

In this proposed design, a control panel may be provided in order for a pilot or operator of a QRAV to access and manipulate a plurality of control parameters for each of the four rotors. The control panel includes inputs in the form of two joysticks and display screens. One of the joysticks may be used by the pilot or operator to control the forward speed $\dot{x}$ by moving the joystick forward and backward, and lateral speed $\dot{y}$ may be controlled by moving it horizontally left and right, while the forward acceleration $\ddot{x}$, or thrust, may be controlled by twisting the joystick. However, in highly maneuvering cases, as in the combat scenario, the pilot can switch the forward speed control to the forward acceleration control. In the acceleration control the forward acceleration $\ddot{x}$ is proportional to the position of the joy stick. The neutral position of the joy stick could cause the aircraft to either hover or maintain its last forward speed. The second joystick may be used to control the rotational movements of the air vehicle. The forward/backward po-

sition may be used to control the pitch of the air vehicle θ, the left/right positions may be used to control the roll ϕ of the air vehicle, while twisting the left joystick 2 may control the yaw angular velocity $\dot{\psi}$.

The touch screen enables the pilot to limit the range of vehicle speed that can be reached by the full span of the joystick. For example in a pick-and-place mission to precisely install bridge construction parts, the range of speed control by the joystick can be limited to 1 or 2 meters per sec for precise motion and control of the air vehicle. Similarly, the pilot can set limits on the vehicle forward acceleration for specific missions. The set up can be saved and retrieved when the pilot starts similar missions. Possible mapping between pilot commands and quadrotor inputs is shown on the table presented in fig.3.

	Activated Control Parameter												
	Action	α1	α2	α3	α4	β1	β2	β3	β4	F1	F2	F3	F4
1	Vertical motion	0°	0°	0°	0°	0°	0°	0°	0°	√	√	√	√
2	*Forward +x direction	+a	0°	+a	0°	90°	0°	90°	0°	-	-	-	-
3	*Backward –x direction	-a	0°	-a	0°	90°	0°	90°	0°	-	-	-	-
4	*Side motion +y	0	+a	0°	+a	0°	0°	0°	0°	-	-	-	-
5	*Side motion -y	0	-a	0°	-a	0°	0°	0°	0°	-	-	-	-
6	Yaw rotation CW	0	+a	0°	-a	0°	0°	0°	0°	-	-	-	-
7	Yaw rotation CCW	0	-a	0°	+a	0°	0°	0°	0°	-	-	-	-
8	Pitch +	0°	0°	0°	0°	0°	0°	0°	0°	↑	-	↓	-
9	Pitch -	0°	0°	0°	0°	0°	0°	0°	0°	↓	-	↑	-
10	Roll +	0°	0°	0°	0°	0°	0°	0°	0°	-	↑	-	↓
11	Roll -	0°	0°	0°	0°	0°	0°	0°	0°	-	↓	-	↑

Figure 3.3: Control commands mapping

The display screens may show information including one or more of: elevation, forward velocity, orientation of the air vehicle (roll, pitch, yaw), odometer, trip meter, fuel level, battery status, global positioning system (GPS) information, and geographic information system (GIS) information. The touchscreen displays and/or the display screens may show information including rotational speed of one or more of the four rotors, power consumption, and alarm status (temperature, overpower, overspeed, etc.).

3.4 Advantages and Simulation Tests

This proposed design can offer many advantages over all the existing designs in the literature. Some of these advantages are tested in this chapter while other are left for future work. For example, not only the motions of quadrotor are decoupled, but also all the translational and rotational speeds can be controlled independent of the positions/orientations. This means that the quadrotor can move on a certain trajectory while maintaining specified speeds and orientations which gives this design superior manoeuvrability. The free inputs can further be used to achieve additional tasks such as overcoming gust disturbances or even as brakes. On the other hand, while the additional inputs may be of great use during critical missions, they can be turned completely off when not needed to save power and reduce control complexity. In fact, the quadrotor is still fully actuated and the motions are completely decoupled using only any two opposite rotors. Failure of any of the rotors would not compromise the safety of the flight or behavior.

Furthermore, if the rotors are allowed to rotate freely in a hemisphere, i.e. α is allowed to reach proper angles; and motors are strong enough, the quadrotor could land safely with only one rotor functioning.

A necessary and sufficient condition for the quadrotor's motions to be decoupled and completely independent with only two opposite rotors running, is that equations (3.4) and (3.5) of forces and moments are independent with only two opposite running. And since the relation between the actual inputs and forces and moments is nonlinear, and it's not convenient to check independence in nonlinear equations, a change of variables is introduced. Let

$$A = C\beta_1 S\alpha_1 \omega_1^2$$

$$B = C\beta_3 S\alpha_3 \omega_3^2$$

$$C = S\beta_1 S\alpha_1 \omega_1^2$$

$$D = S\beta_3 S\alpha_3 \omega_3^2$$

$$E = C\alpha_1 \omega_1^2$$

$$F = C\alpha_3 \omega_3^2$$

Those variables (A through F) can be manipulated freely and independently. That's to say, one can find proper values of β, α and ω that produce any arbitrary values of the variables A through F. To prove that, take the equations of A, C and E where they share the same input variables α_1, ω_1 and β. For any arbitrary

values of A and C, the ratio $\frac{A}{C} = \frac{C\beta_1}{S\beta_1}$ Determines the value of the variable β_1. The other two variables are determined by the values of either A or C and the value of E (the ratio $\frac{A}{C}$ is already determined hence fixing one variable will automatically fix the other). Now, Rewriting the equation of forces and moments (3.4) and (3.5) with the new variables and with only rotors 1 and 3 running:

$$\begin{bmatrix} F_x \\ F_y \\ F_z \end{bmatrix} = b \begin{bmatrix} A+B \\ C+D \\ E+F \end{bmatrix} \tag{3.11}$$

$$\begin{bmatrix} M_x \\ M_y \\ M_z \end{bmatrix} = \begin{bmatrix} d(A-B) & +bh(C+D) \\ d(C-D) & -bh(A+D) & +bl(F-E) \\ d(E-F) & +bl(C-D) \end{bmatrix} \tag{3.12}$$

Combining the two equations

$$\begin{bmatrix} F_x \\ F_y \\ F_z \\ M_x \\ M_y \\ M_z \end{bmatrix} = \begin{bmatrix} b & b & 0 & 0 & 0 & 0 \\ 0 & 0 & b & b & 0 & 0 \\ 0 & 0 & 0 & 0 & b & b \\ d & -d & bh & bh & 0 & 0 \\ -bh & b & d & -d-bh & -bl & bl \\ 0 & 0 & bl & -bl & d & -d \end{bmatrix} \begin{bmatrix} A \\ B \\ C \\ D \\ E \\ F \end{bmatrix} \tag{3.13}$$

This matrix is full rank. Which means that the forces and moments are independent and there's always a combination of variables A through F that produce any arbitrary values of forces and moments with only two rotors running.

Considering the aforementioned advantages, this design can serve for many critical applications. The fact that the motions are completely decoupled and that the quadrotor doesn't need to pitch to go forward nor to roll for lateral motions; this fact makes the quadrotor very suitable for sensitive payload as it provides a very smooth ride. Surveillance and monitoring could be improved as the quadrotor can fly at precise attitudes with precise speeds and orientations. This can be very suitable for military applications.

In the following subsections, several maneuvers are simulated to test the decoupling of motions and fault tolerance. The rotational friction is assumed to be zero during all simulations. It's important to point out that the objective here is not to design a high performance controller but instead, a simple controller that

will be able to highlight the advantages mentioned in this chapter. To achieve this with lowest complexity, trivial pairings are done between inputs and outputs. The four propellers' speeds ω_i's are paired with the quadrotor elevation z. The four speeds are set to be equal and are given the notion ω_z.

In addition, the angles α_2 and α_4 of rotors 2 and 4 respectively are paired with the velocity along x-axis. The two angles are set to be equal and are given the notion α_x. While the angles α_1 and α_3 of rotors 1 and 3 respectively are paired with the velocity along y-axis. Similarly, these two angles are set to be equal and are given the notion α_y .

The rest of the inputs and states will be ignored at this stage. The control scheme used is a simple Proportional-Integral (PID) controller with partial state feedback.

Let e_z, $e_{\dot{x}}$ and $e_{\dot{y}}$ be the error in elevation, error in velocity along the x-axis and error in velocity along the y-axis respectively. And let

$$U_C = [w_z \quad \alpha_z \quad \alpha_y]^T$$

$$e = [e_z \quad e_{\dot{x}} \quad e_{\dot{y}}]^T$$

$$K_P = \begin{bmatrix} K_P1 & 0 & 0 \\ 0 & K_P2 & 0 \\ 0 & 0 & K_P3 \end{bmatrix}$$

$$K_I = \begin{bmatrix} K_I1 & 0 & 0 \\ 0 & K_I2 & 0 \\ 0 & 0 & K_I3 \end{bmatrix}$$

$$K_D = \begin{bmatrix} K_D1 & 0 & 0 \\ 0 & K_D2 & 0 \\ 0 & 0 & K_D3 \end{bmatrix}$$

Then, the PID controller is defined as follows

$$U_C = K_P e + K_I \int e \, \mathrm{d}t + K_D \frac{de}{dt} \tag{3.14}$$

The constants used in the simulations are listed below

* These values were taken from [31]

Table 3.1: Values of medel and controller parameters

$g = 9.8$	$b^* = 2.92e-6$	$d^* = 1.12e-7$
$m^* = 0.5$	$l^* = 0.2$	$h = 0$
$\omega_{max} = (10000)\frac{2\pi}{60}$	$I_x^* = 4.85e-3$	$I_y^* = 4.85e-3$
$I_z^* = 4.81e-3$	$K_1 = \frac{1}{2} b \frac{\omega_{max}^2}{40}$	$K_2 = \frac{1}{2} b \frac{\omega_{max}^2}{40}$
$K_3 = b\frac{\omega_{max}^2}{40}$	$K_P1 = 20$	$K_p2 = 1e-4$
$K_p3 = 1e-4$	$K_I1 = 5e-2$	$K_I2 = 5e-5$
$K_I3 = 5e-5$	$K_D1 = 1000$	$K_D2 = K_D3 = 0$

3.4.1 Decoupling

This subsection presents three flight simulations to demonstrate decoupling of motions. The objective of these three tests is to observe how the quadrotor can follow arbitrary trajectories with specific motions without compromising other motions and/or orientations.

In the first flight, the quadrotor elevates up to $10m$ and then moves laterally with a velocity of $10m/s$, Fig 3.4 - 3.7. Fig 3.4 shows the x, y and z positions where it's evident that the quad achieved the vertical position of $10m$. In Fig 3.5, it can be seen that the lateral velocity $\dot{y}$ is achieved while all the orientation angles shown in Fig 3.6 are kept fixed at zero. Fig 3.7 shows the input angle α in rotors 2 and 4 that are manipulated to achieve this mission.

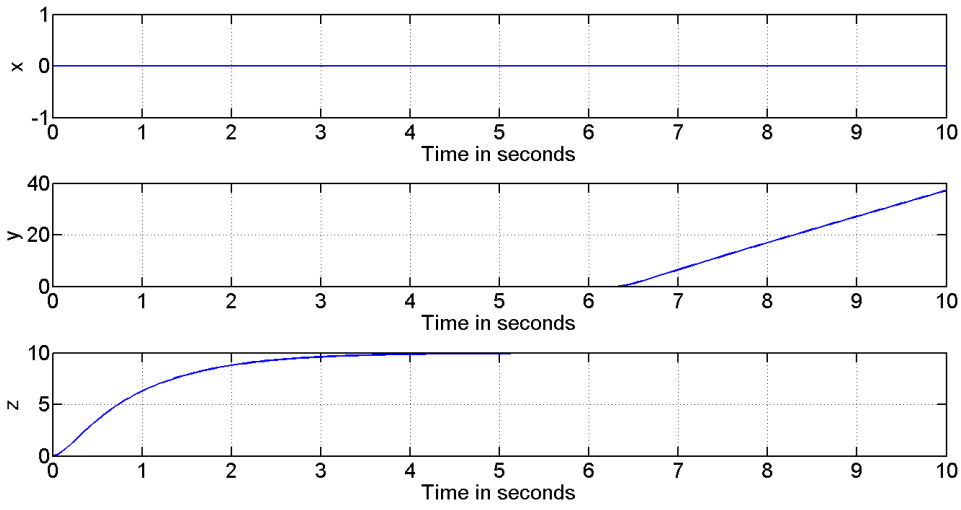

Figure 3.4: Flight 1, x, y and z positions

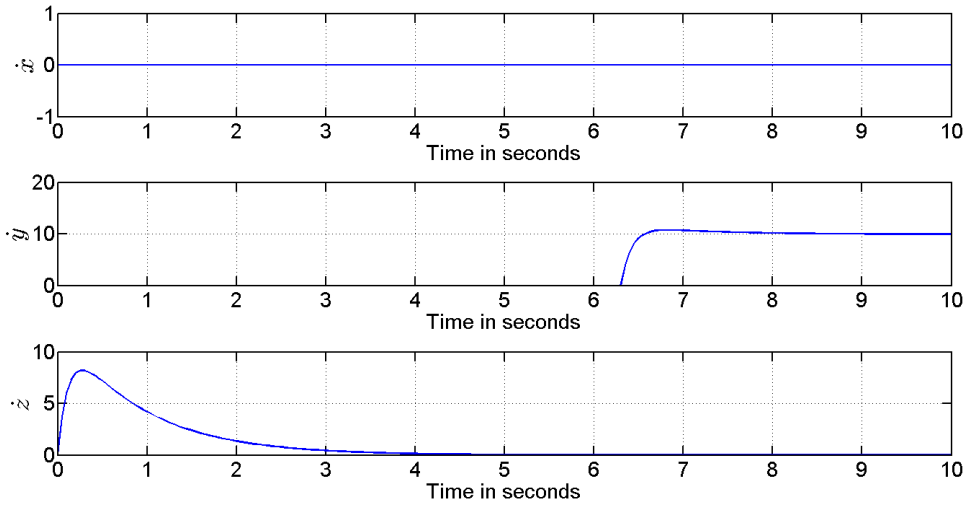

Figure 3.5: Flight 1, velocities $\dot{x}$, $\dot{y}$ and $\dot{z}$

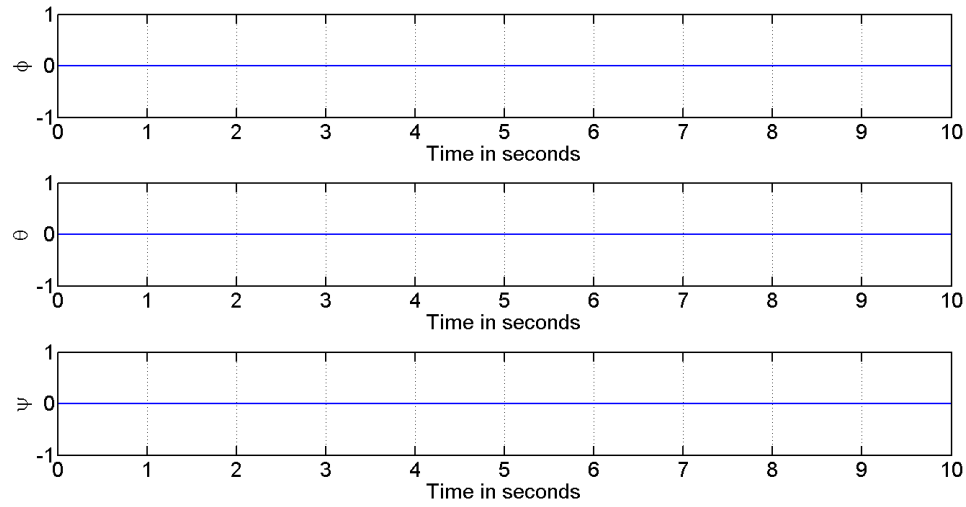

Figure 3.6: Flight 1, The three orientation angles Φ, Θ and Ψ

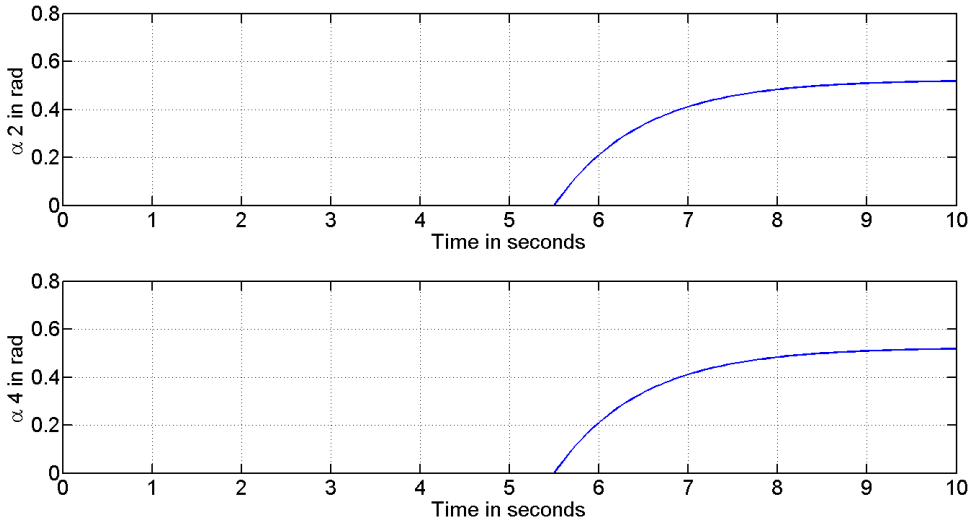

Figure 3.7: Flight 1, Rotors 2 and 4 α rotation angle; $\beta = 0$

In the second flight, the quadrotor elevates to 50 meters, and while it's still elevating it's commanded to thrust forward with a speed of $5m/s$. Similar to the figures in the first flight test, Fig 3.8 - 3.10 show that the desired positions, velocities and orientation angles are achieved independently.

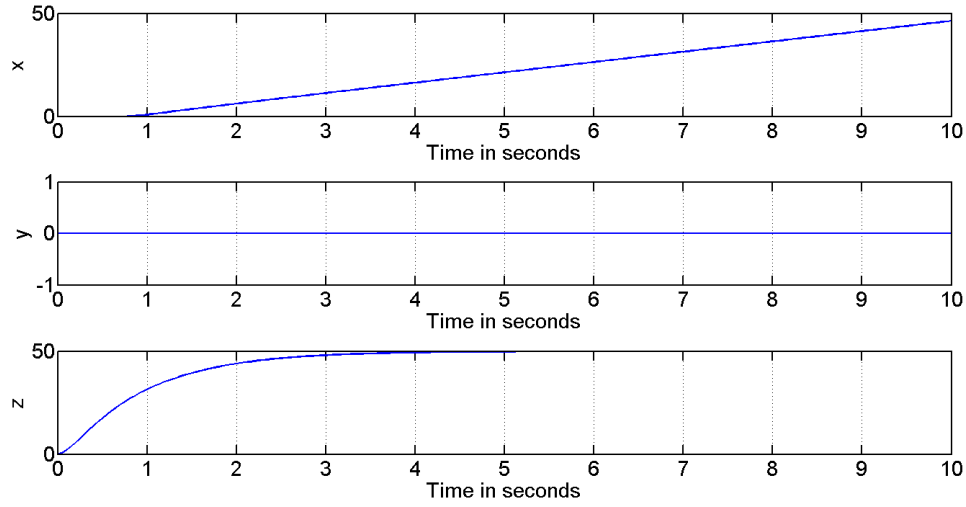

Figure 3.8: Flight 2, x, y and z positions

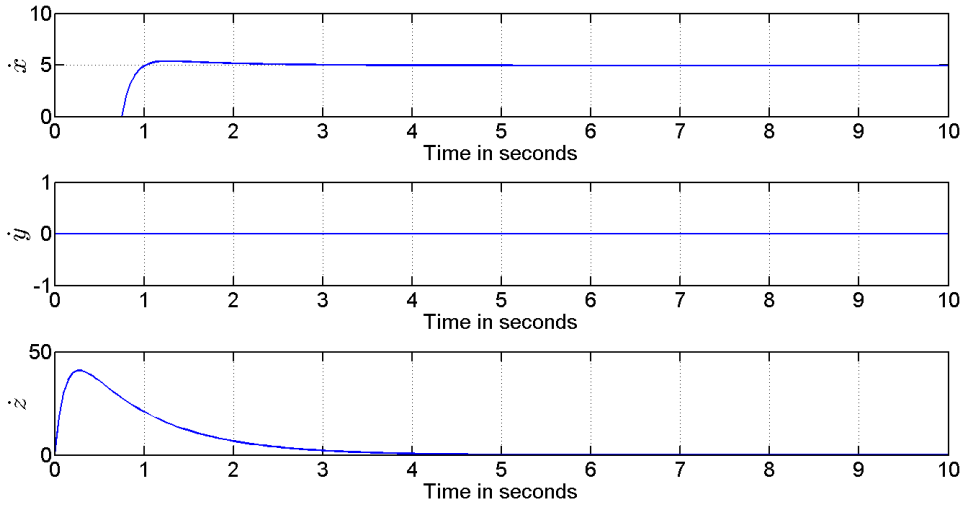

Figure 3.9: Flight 2, velocities $\dot{x}$, $\dot{y}$ and $\dot{z}$

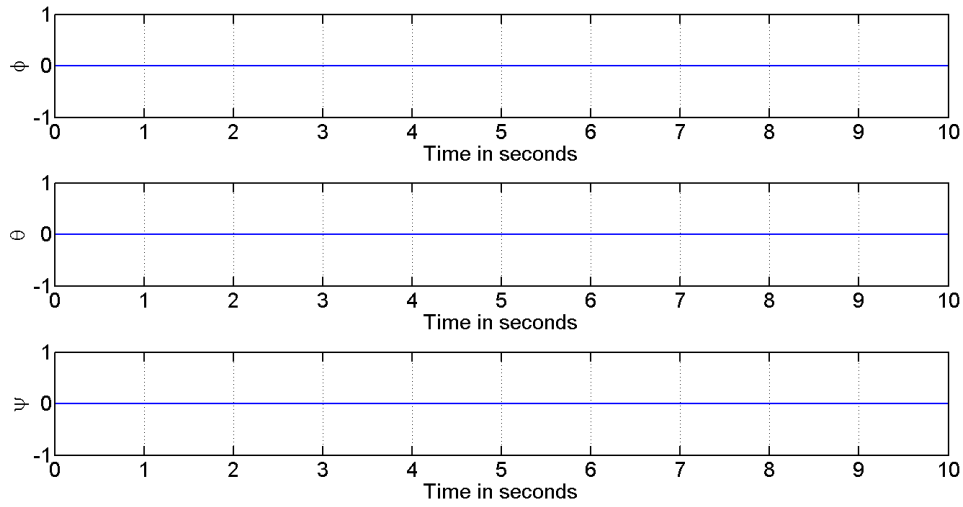

Figure 3.10: Flight 2, The three orientation angles Φ, Θ and Ψ

In the third flight test, the quadrotor is commanded to hover, then thrust move laterally with a constant speed of $10m/s$, which is the same as flight 1, except that this time the quad has to maintain a constant pitch angle of $\pi/6$. The results of

this flight are shown in Fig 3.11 - 3.13. This is a very strong test as the results in the figures show that not only can follow certain translational trajectories while keeping orientation angles undisturbed, but also can achieve desired orientation angles completely independently of its translational path.

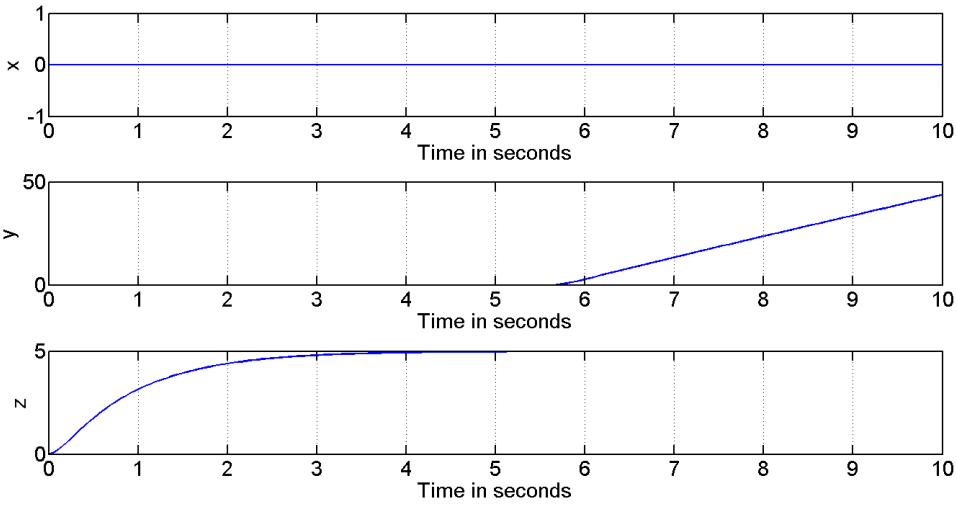

Figure 3.11: Flight 3, Flight 1, x, y and z positions

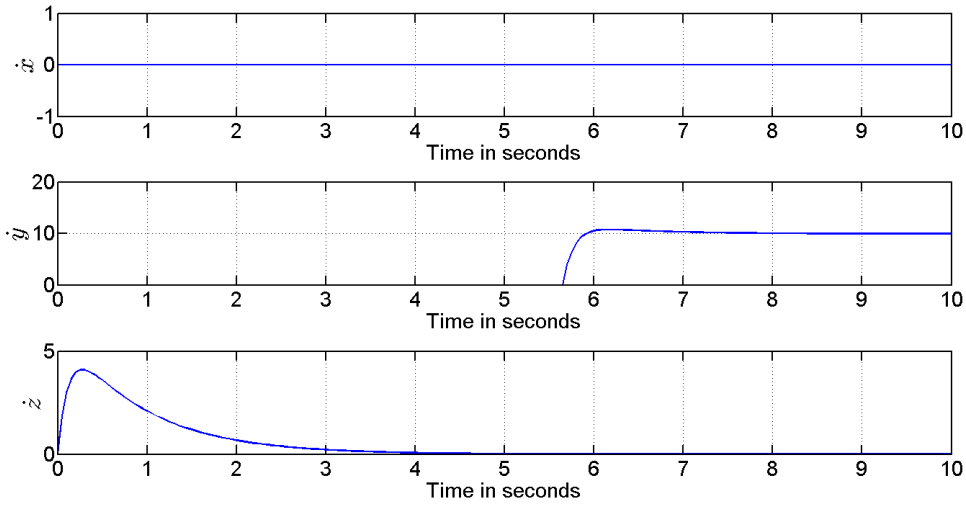

Figure 3.12: Flight 3, velocities $\dot{x}$, $\dot{y}$ and $\dot{z}$

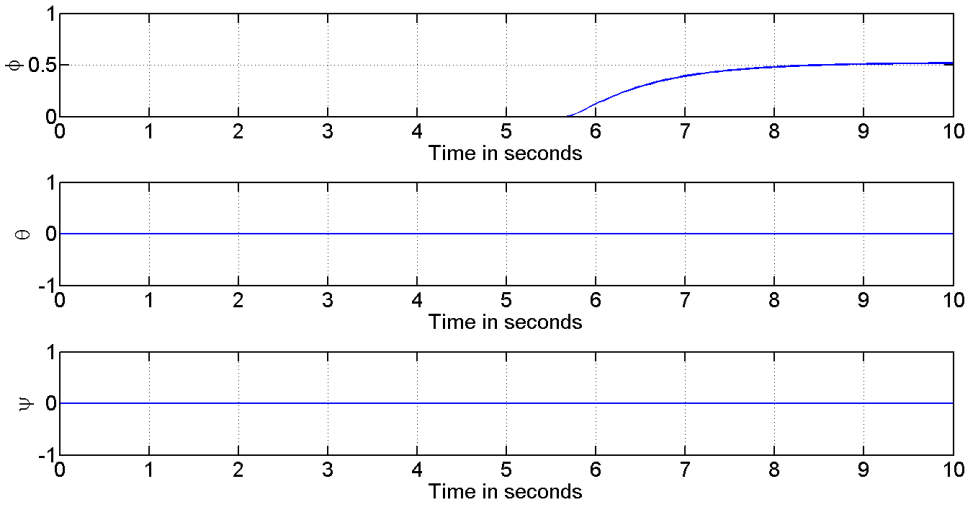

Figure 3.13: Flight 3, The three orientation angles Φ, Θ and Ψ

Three important observations can be made form the simulation results. Firstly, It's evident that thrusting forward didn't compromise the vertical position of the quadrotor. The second observation is that in both flight 1 and 2, the three orientation angles, Φ, Θ and Ψ remained unchanged. This is a very important result as it shows the smoothness of the flight and the absence of perturbation. Finally, flight 3 shows that control objectives were carried out simultaneously and independently while maintaining other motions undisturbed.

3.4.2 Fault Tolerance

During the fourth flight, two rotors (rotors 1 and 3) are assumed to be faulty (or turned off). The control scheme has to be modified because of this actuator loss. The modification here is simple, instead of manipulating α_y to control the velocity along the y-axis, α_x is used as input with β_2 and β_4 are set to $\pi/2$.

With only two rotors remaining (rotor 2 and 4), The quadrotor is commanded to perform a similar flight to the first from the previous section. It's set to elevates up to $200m$ and then thrust forward with a fixed velocity of $30m/s$. Fig 3.14 - 3.18 show the response. The figures show the positions, velocities and orientation angles respectively. Again, it's evident that the control objectives are still achieved independently of each other with only two rotors running. Fig 3.17 shows α angles in rotors 2 and 4 while Fig 3.18 shows the speeds of the four rotors where it's clear that only rotor 2 and 4 are running.

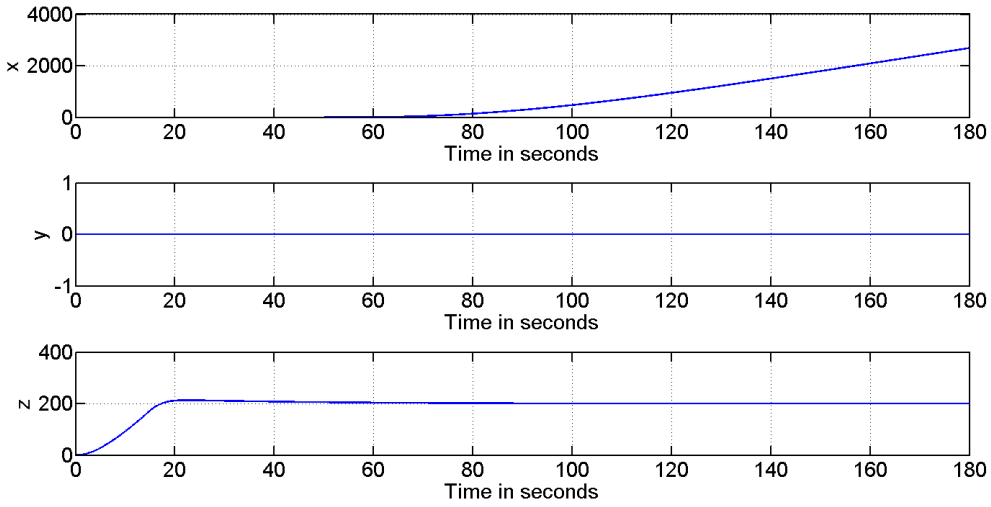

Figure 3.14: Flight 4, x, y and z positions

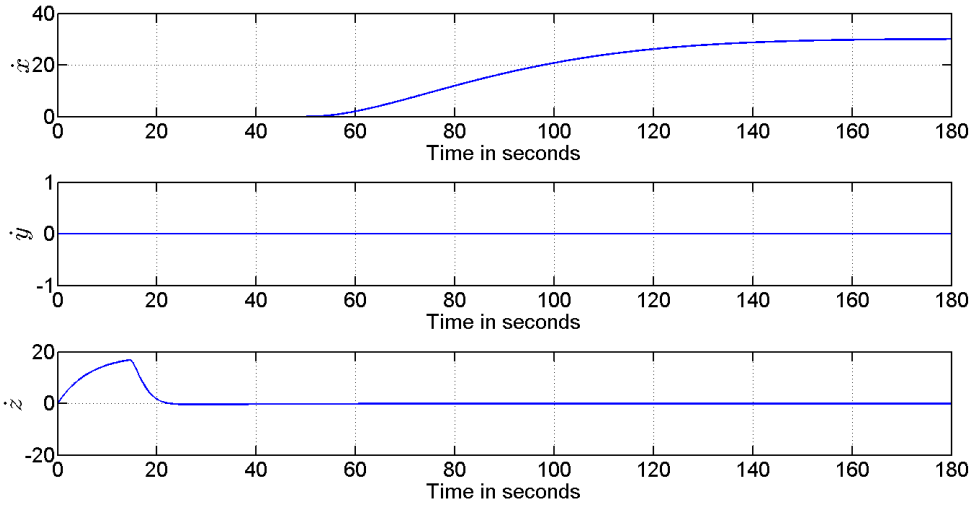

Figure 3.15: Flight 4, velocities $\dot{x}$, $\dot{y}$ and $\dot{z}$

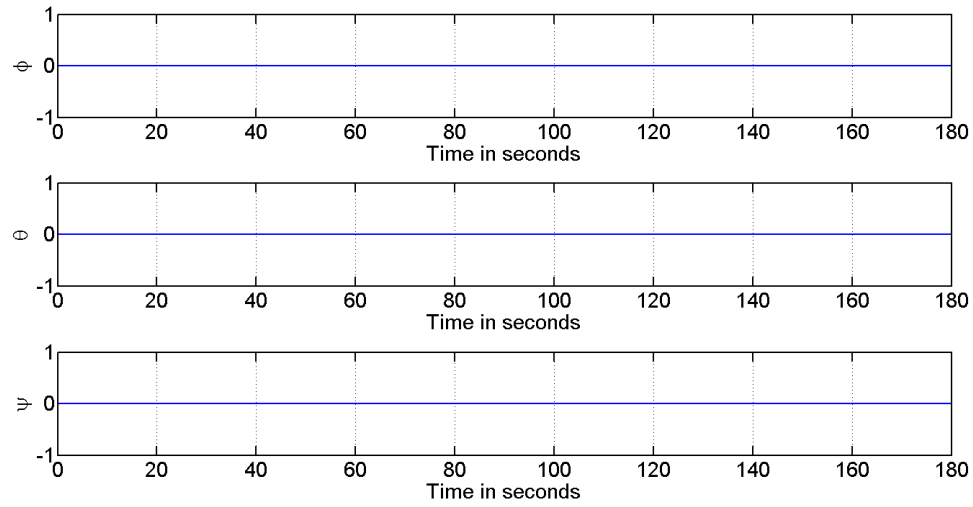

Figure 3.16: Flight 4, The three orientation angles Φ, Θ and Ψ

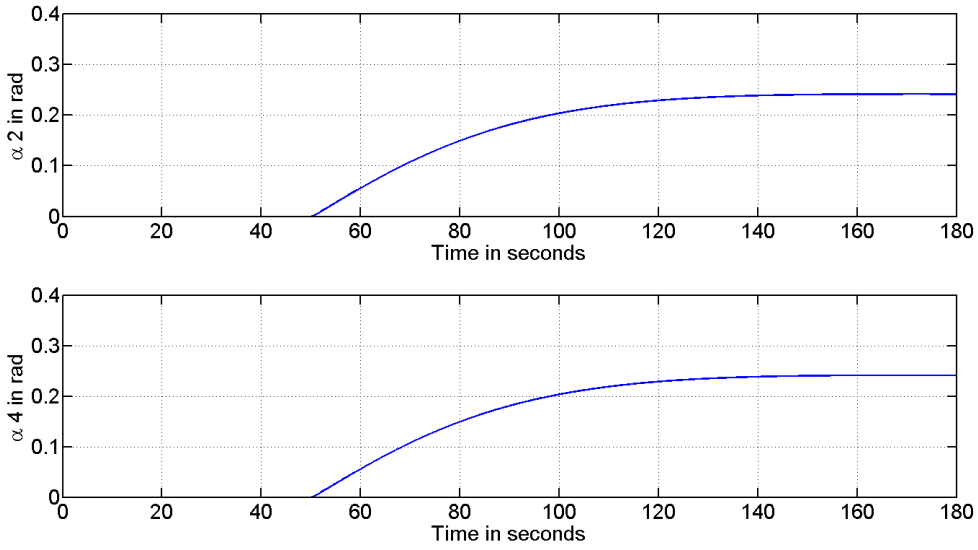

Figure 3.17: Flight 4, Rotors 2 and 4 α rotation angle; $\beta = 0$

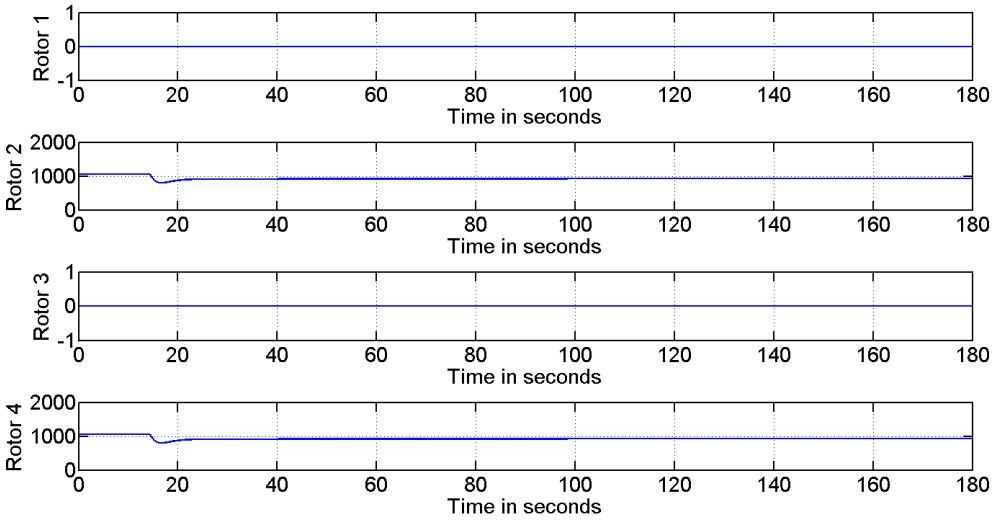

Figure 3.18: Flight 4, the four rotors speeds

The simulation shows clearly that only two rotors are enough to control and decouple the outputs of the system. In fact, with only two rotors running, six inputs are available which means that the system is fully actuated and

suitable for conventional missions. This result is important because it means that not only the quadrotor is tolerant to losing half of its actuators, but also can save energy by turning them off for ordinary missions that don't require high manoeuvrability.

3.5 Conclusion

This paper presented a proposed design for quadrotor. The mathematical model is presented based on Newton-Euler formulation. The proposed quadrotor has all of its rotors allowed to tilt with two degrees of freedom w.r.t the fixed body frame. With this addition of 8 inputs, the system is fully actuated and capable of tracking more outputs separately and independently (6 positions/orientations and 6 translational/rotational speeds). This improves maneuverability and agility of quadrotor and enhances fault tolerance capabilities. In fact, the system was proven to be completely operational with only any two opposite rotors running. Several flight simulations were carried out. The simulations demonstrated some of the advantages of this design over the conventional quadrotor such as complete decoupling of motions, energy saving, ability to track arbitrary trajectories for all outputs independently, robustness and tolerance against various failures.

CHAPTER 4

FEEDBACK LINEARIZATION CONTROL

4.1 Introduction

Feedback linearization is one of the very well known techniques to deal with nonlinear systems. It is simple in the sense that nonlinearities are removed through the inputs of the system. It can be very effective for systems with relatively high modeling accuracy, which is the case here. As mentioned in Chapter 2, Feedback Linearization has been extensively used in the literature to control quadrotors. However, two main differences arise when dealing with the new proposed system. The first difference is that the inputs are related to each other and to the states in a highly nonlinear manner which prevents conventional feedback linearization where the system has to be linear in inputs. To overcome these obstacles, a change of inputs is introduced. The second difference is the fact that the proposed system

has more inputs than states. This leads to infinite combinations of inputs for any desired maneuver. To choose the best set of inputs, optimization is introduced after the controller.

This Chapter is organized as follows: section 4.2 presents control problem formulation where feedback linearization technique is carried out step by step. Section 4.3 demonstrates analysis of the control technique. Section 4.4 presents the results of simulating this technique whereas section 4.5 concludes the chapter.

4.2 Controller design

4.2.1 Problem Formulation

A quick preview of the modeling chapter reveals that the system presented has more inputs than degrees of freedom; that's to say, it's overactuated. Taking that into account, it might be desirable to find six control inputs -forces and moments- that reflect a direct effect on the six degrees of freedom. The choice that's most related to the degrees of freedom is the set of forces and moments along the three axes. Let $F_v = [F_x \quad F_y \quad F_z]^T$ and $M_v = [M_x \quad M_y \quad M_z]^T$ be the control inputs which are related to the actual 12 inputs through the following static equations:

$$\begin{bmatrix} F_x \\ F_y \\ F_z \end{bmatrix} = \sum_{i=1}^{4} F_i \tag{4.1}$$

$$\begin{bmatrix} M_x \\ M_y \\ M_z \end{bmatrix} = \sum_{i=1}^{4} M_i \tag{4.2}$$

Note that the 6 control inputs $[F_x \quad F_y \quad F_z \quad M_x \quad M_y \quad M_z]$ are composed of nonlinear combination of 12 actual inputs $[\omega_i \quad \alpha_i \quad \beta_i], i = 1, ..., 4$. This means that for each set of control inputs, the system has infinitely many combinations of actual inputs. The way to find the best combination is discussed in the next section.

Re-writing equations (3.6) and (3.7) in terms of the new control inputs:

$$m \begin{bmatrix} \ddot{x} \\ \ddot{y} \\ \ddot{z} \end{bmatrix} = \begin{bmatrix} 0 \\ 0 \\ -mg \end{bmatrix} - \begin{bmatrix} K_1\dot{x} \\ K_2\dot{y} \\ K_3\dot{z} \end{bmatrix} + R_B^E \begin{bmatrix} F_x \\ F_y \\ F_z \end{bmatrix} \tag{4.3}$$

$$I \begin{bmatrix} \dot{p} \\ \dot{q} \\ \dot{r} \end{bmatrix} = -(\begin{bmatrix} p \\ q \\ r \end{bmatrix} \times I \begin{bmatrix} p \\ q \\ r \end{bmatrix}) - M_G + \begin{bmatrix} M_x \\ M_y \\ M_z \end{bmatrix} \tag{4.4}$$

For convenience, the equations of forces and moments will be treated as two different subsystems for the rest of our analysis where equation (4.3) represents subsystem 1 and (4.4) represents subsystem 2.

To construct the formulation of feedback linearization for tracking problem for subsystem 1, let

$$e_\eta = \eta_d - \eta$$

where η is the position vector, η_d is the desired position vector and e_η is the error in position. Dividing by m and subtracting $\ddot{\eta}_d$ from both sides of equation (4.3)

$$\ddot{\eta} - \ddot{\eta}_d = g_z - (K/m)\dot{\eta} + (R_B^E/m)F - \ddot{\eta}_d$$

Rearranging for $e_\eta = \eta_d - \eta$

$$\ddot{e}_\eta = -g_z + (K/m)\dot{\eta} - (R_B^E/m)F + \ddot{\eta}_d \tag{4.5}$$

To introduce feedback linearization for this part of the system through the control input F_v, Let:

$$F_v = m(R_B^E)^{-1}(-g_z + (K/m)\dot{\eta} + \ddot{\eta}_d + K_{vF}\dot{e}_\eta + K_{pF}e_\eta) \tag{4.6}$$

Substituting F_v into F in equation (4.5) produces

$$\ddot{e}_\eta = -K_{vF}\dot{e}_\eta - K_{pF}e_\eta \tag{4.7}$$

where K_{vF} and K_{pF} are control variables to be chosen in such a way that the error

e_η goes to zero.

A similar procedure is carried out for subsystem 2. Let

$$e_\Omega = \Omega_d - \Omega$$

where Ω is the body angular velocity vector, Ω_d is the desired body angular velocity vector and e_η is the error in body angulr velocity. Pre-multiplying by I^{-1} and subtracting $\dot{\Omega}_d$ from both sides of equation (4.4)

$$\dot{\Omega} - \dot{\Omega}_d = -I^{-1}(\Omega \times I\Omega) - I^{-1}M_G + I^{-1}M - \dot{\Omega}_d$$

Rearranging for $e_\Omega = \Omega_d - \Omega$

$$\dot{e}_\Omega = I^{-1}(\Omega \times I\Omega) + I^{-1}M_G - I^{-1}M + \dot{\Omega}_d \tag{4.8}$$

To introduce feedback linearization for this part of the system through the control input M_v, Let:

$$M_v = (\Omega \times I\Omega) + I\dot{\Omega}_d + M_G + IK_{vM}e_\Omega + IK_{pM}\int e_\Omega \,\mathrm{d}t \tag{4.9}$$

Substituting M_v into M in equation (4.8) produces

$$\dot{e}_\Omega = -K_{vM}e_\Omega - K_{pM}\int e_\Omega \,\mathrm{d}t \tag{4.10}$$

where $\int e_\Omega \,\mathrm{d}t$ denotes the error in orientation, K_{vM} and K_{pM} are control constant.

The choice of actual inputs that produce the new control inputs is discussed in the optimization section. Fig. (4.1) shows an overall block diagram of the system with the controller.

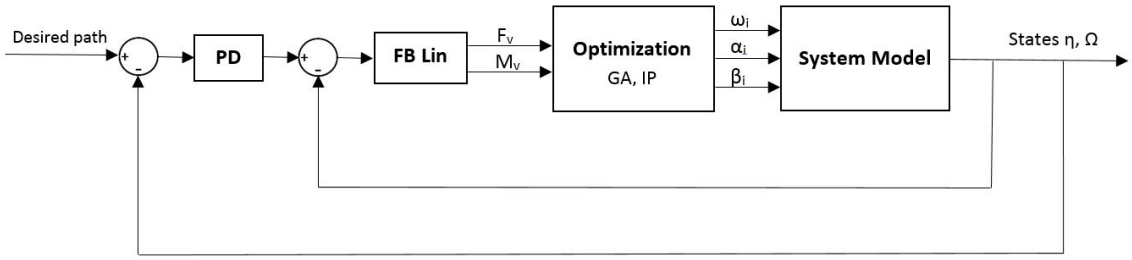

Figure 4.1: Block Diagram of the Control Architecture

4.2.2 Analysis

In this subsection, the stability of the system is studied under two different assumptions.

Theorem 4.1 *Under the assumption of known system dynamics, subsystems 1 and 2 are asymptotically stable under control inputs (4.6) and (4.9) respectively with two conditions*

- $K_{pF} = K_{pM} = I$, *where* I *here is the identity matrix.*
- K_{vF} *and* K_{vM} *are positive definite matrices*

Proof.

For subsystem1, choose the Lyaponov function

$$V(e_\eta) = 1/2(e_\eta^T e_\eta + \dot{e_\eta}^T \dot{e}_\eta) \qquad \geq 0 \tag{4.11}$$

Then

$$\begin{aligned}\dot{V}(e_\eta) &= e_\eta^T \dot{e}_\eta + \dot{e}_\eta^T \ddot{e}_\eta \\ &= \dot{e}_\eta^T e_\eta + \dot{e}_\eta^T \ddot{e}_\eta \\ &= \dot{e}_\eta^T (e_\eta + \ddot{e}_\eta) \\ &= \dot{e}_\eta^T [e_\eta - g_z - (K/m)\dot{\eta} - (R_B^E/m)F + \ddot{\eta}_d]\end{aligned} \tag{4.12}$$

A sufficient and necessary condition for the error e_{eta} to be locally stable is that $\dot{V}(e_{eta}) \quad \leq 0$. To check this condition, the linearization controller is introduced through the input F_v

$$F_v = m(R_B^E)^{-1}(-g_z + (K/m)\dot{\eta} + \ddot{\eta}_d + K_{vF}\dot{e}_\eta + e_\eta) \tag{4.13}$$

Substituting F_v into F in equation (4.12) yields

$$\dot{V}(e_\eta) = -K_{vF}\dot{e}_\eta^T \dot{e}_\eta \qquad \leq 0 \tag{4.14}$$

Comparing the expressions of F_v in equation (4.13) and (4.6) yields $K_{pF} = I$ while K_{vF} is a positive definite matrix.

For subsystem2, choose the Lyaponov function

$$V(e_\Omega) = 1/2(\int e_\Omega^T \int e_\Omega + \dot{e_\Omega}^T e_\Omega) \qquad \geq 0 \tag{4.15}$$

Then

$$\begin{aligned}\dot{V}(e_\Omega) &= \int e_\Omega^T e_\Omega + e_\Omega^T \dot{e}_\Omega \\ &= e_\Omega^T \int e_\Omega + e_\Omega^T \dot{e}_\Omega \\ &= e_\Omega^T (\int e_\Omega + \dot{e}_\Omega) \\ &= e_\Omega^T [\int e_\Omega + (I^{-1}\Omega \times \Omega) + I^{-1} M_G - I^{-1} M + \ddot{\Omega}_d]\end{aligned} \tag{4.16}$$

Similarly, to check the stability condition, the feedback linearization controller is introduced through the input M_v

$$M_v = (\Omega \times I\Omega) - I\dot{\Omega} + M_G + IK_{vM}\dot{e}_\Omega + I\int e_\Omega \tag{4.17}$$

Substituting M_v into M in equation (4.16)

$$\dot{V}(e_\eta) = -K_{vM} e_\Omega^T e_\Omega \qquad \leq 0 \tag{4.18}$$

Similarly again, Comparing the expression of F in equation (4.17) with F_v in equation (4.9) yields $K_{pM} = I$ while K_{vM} is a positive definite matrix.

∎

Theorem 4.2 *Under the assumption that the drag constant K is not known exactly and is estimated with $\hat{K}$, subsystem 1 is asymptotically stable with the conditions*

- $K_{pF} = K_{pM} = I$ *where I here is the identity matrix*

- *K_{vF} and K_{vM} are positive definite matrices*

- *Drag constant K is estimated with $\hat{K}$ through an adaptive estimator, where*

$$\dot{\hat{K}} = \begin{bmatrix} \frac{\dot{e}_{(1)}\dot{\eta}_{(1)}}{m} & 0 & 0 \\ 0 & \frac{\dot{e}_{(2)}\dot{\eta}_{(2)}}{m} & 0 \\ 0 & 0 & \frac{\dot{e}_{(3)}\dot{\eta}_{(3)}}{m} \end{bmatrix}$$

Proof.

The drag constant appears only in subsystem 1. Choose the Lyaponov function

$$V(e_\eta, \tilde{K}) = 1/2(e_\eta^T e_\eta + \dot{e_\eta}^T \dot{e}_\eta) + s^T \tilde{K}^T \tilde{K} s \qquad \geq 0 \tag{4.19}$$

where $s = [1 \quad 1 \quad 1]^T$ and $\tilde{K} = \hat{K} - K$.

Then

$$\begin{aligned} \dot{V}(e_\eta, \tilde{K}) &= e_\eta^T \dot{e}_\eta + \dot{e}_\eta^T \ddot{e}_\eta + s^T \tilde{K}^T \dot{\tilde{K}} s \\ &= \dot{e}_\eta^T e_\eta + \dot{e}_\eta^T \ddot{e}_\eta + s^T \tilde{K}^T \dot{\tilde{K}} s \\ &= \dot{e}_\eta^T (e_\eta + \ddot{e}_\eta) + s^T \tilde{K}^T \dot{\tilde{K}} s \\ &= \dot{e}_\eta^T [e_\eta - g_z - (K/m)\dot{\eta} - (R_B^E/m)F + \ddot{\eta}_d] + s^T \tilde{K}^T \dot{\tilde{K}} s \end{aligned} \tag{4.20}$$

But $\dot{\tilde{K}} = \dot{\hat{K}} - \dot{K}$. And since K is constant, this yields $\dot{\tilde{K}} = \dot{\hat{K}}$. Substituting in $\dot{V}(e_\eta, \tilde{K})$

$$\dot{V}(e_\eta, \tilde{K}) = \dot{e}_\eta^T[e_\eta - g_z - (K/m)\dot{\eta} - (R_B^E/m)F + \ddot{\eta}_d] + s^T\tilde{K}^T\dot{\hat{K}}s \tag{4.21}$$

Introducing the feedback linearization controller through the input F

$$F = m(R_B^E)^{-1}(-g_z + (\hat{K}/m)\dot{\eta} + \ddot{\eta}_d + K_{vF}\dot{e}_\eta + e_\eta) \tag{4.22}$$

Substituting in $\dot{V}(e_\eta, \tilde{K})$

$$\dot{V} = -K_{vF}(\dot{e}_\eta^T\dot{e}_\eta) - \dot{e}_\eta^T\frac{\tilde{K}}{m}\dot{\eta} + s^T\tilde{K}^T\dot{\tilde{K}}s \tag{4.23}$$

Note that $\tilde{K}$ and $\dot{\hat{K}}$ are 3x3 diagonal matrices while $\dot{e}$ and $\dot{\eta}$ are 3x1 matrices. To analyze the second term of the equation further, the matrices are broken down to their basic elements

$$\begin{aligned}
&\dot{e}_\eta^T\frac{\tilde{K}}{m}\dot{\eta} + s^T\tilde{K}^T\dot{\tilde{K}} = \\
&-\frac{1}{m}[\dot{e}_{(1)}\tilde{K}_{(1,1)}\dot{\eta}_{(1)} + \dot{e}_{(2)}\tilde{K}_{(2,2)}\dot{\eta}_{(2)} + \dot{e}_{(3)}\tilde{K}_{(3,3)}\dot{\eta}_{(3)}] \\
&+ [\tilde{K}_{(1,1)}\dot{\tilde{K}}_{(1,1)} + \tilde{K}_{(2,2)}\dot{\tilde{K}}_{(2,2)} + \tilde{K}_{(3,3)}\dot{\tilde{K}}_{(3,3)}] \\
&= \tilde{K}_{(1,1)}[\dot{\tilde{K}}_{(1,1)} - \frac{\dot{e}_{(1)}\dot{\eta}_{(1)}}{m}] + \tilde{K}_{(2,2)}[\dot{\tilde{K}}_{(2,2)} - \frac{\dot{e}_{(2)}\dot{\eta}_{(2)}}{m}] \\
&+ \tilde{K}_{(3,3)}[\dot{\tilde{K}}_{(3,3)} - \frac{\dot{e}_{(3)}\dot{\eta}_{(3)}}{m}]
\end{aligned} \tag{4.24}$$

To set this part equal to zero, let

$$\dot{\hat{K}} = \begin{bmatrix} \frac{\dot{e}_{(1)}\dot{\eta}_{(1)}}{m} & 0 & 0 \\ 0 & \frac{\dot{e}_{(2)}\dot{\eta}_{(2)}}{m} & 0 \\ 0 & 0 & \frac{\dot{e}_{(3)}\dot{\eta}_{(3)}}{m} \end{bmatrix}$$

Substituting $\dot{\hat{K}}$ in equation (4.23)

$$\dot{V} = -K_{vF}(\dot{e}_{\eta}^{T}\dot{e}_{\eta}) \qquad \leq 0 \tag{4.25}$$

4.3 Optimization

4.3.1 Introduction

Optimization is the process of selecting the best (optimum) element -or set of elements- from a set of available alternatives according to some preset criteria. In the situation presented here, it is a question of finding the best -according to some cost function- combination of inputs that satisfy the control equations.

As mentioned in the previous section, the forces F and moments M are used as inputs to the system to avoid dealing with the nonlinearity present in the actual inputs ω_i, α_i and β_i. Feedback linearization control is also achieved through F

and M which means that the controller chooses values of F and M to be fed as inputs to the system. It has been also shown in chapter 3 that with only two opposite rotors running, there's always a combination of ω_i, α_i and β_i that satisfy any arbitrary values of F and M. This means that with full actuation, there's an infinite combinations of ω_i, α_i and β_i that satisfy any arbitrary values of F and M. The question addressed in this section is how to choose one combination of ω_i, α_i and β_i from the set of infinitely many combinations.

Several optimization techniques are available in the literature. However, few of them deal with nonlinear problem with constraints. Choosing the suitable optimization technique from the set of available ones could be thought of as an optimization problem by itself, however, this is out of the scope of this research. Two optimization techniques are tested and compared as a proof of concept and to complete the controller design discussed in the previous section. This part specifically has high potential for improvement in both theory and implementation.

It must be clear that this is not a typical optimal control problem where the objective is to find optimal gains for the controller, instead, the controller gains are already determined and the purpose of optimization is to map the forces and moments used in the controller to the actual 12 inputs of the system through the static equations relating them.

4.3.2 Problem Formulation

It's first desired to find a cost function for the optimization problem, which means finding some criteria to choose among the infinitely many sets of inputs. The most typical and critical objective in UAV application is the minimization of energy consumption during the flight. The cost function can be written as follow

$$J(\omega, \alpha, \beta) = \sum_{i=1}^{n} \left\{ w_1 \sum_{i=1}^{4} \omega_i^3 + w_2 \sum_{i=1}^{4} (\Delta\alpha_i)^2 + w_3 \sum_{i=1}^{4} (\Delta\beta_i)^2 \right\}$$

where the first term is the power consumption by the rotors. The cubic exponent comes from the assumption that the torque is proportional to the square of the angular velocity, while the power is the torque time the angular velocity. The second and the third penalize tilting movements (cost of energy) and n is the number of samples over which the optimization is performed.

The optimization problem can then be written as follows

$$min \quad J(\omega, \alpha, \beta)$$

Subject to

$$\begin{bmatrix} F_{x(j)} \\ F_{y(j)} \\ F_{z(j)} \end{bmatrix} = \sum_{i=1}^{4} \begin{bmatrix} 0 & 0 & C\beta_{(i,j)} S\alpha_{(i,j)} \\ 0 & 0 & S\beta_{(i,j)} S\alpha_{(i,j)} \\ 0 & 0 & C\alpha_{(i,j)} \end{bmatrix} \begin{bmatrix} 0 \\ 0 \\ b\omega_{(i,j)}^2 \end{bmatrix} \quad j = 1, ..., n$$

$$\begin{bmatrix} M_{x(j)} \\ M_{y(j)} \\ M_{z(j)} \end{bmatrix} = \sum_{i=1}^{4} \begin{bmatrix} 0 & 0 & C\beta_{(i,j)}S\alpha_{(i,j)} \\ 0 & 0 & S\beta_{(i,j)}S\alpha_{(i,j)} \\ 0 & 0 & C\alpha_{(i,j)} \end{bmatrix} \begin{bmatrix} 0 \\ 0 \\ d\omega^2_{(i,j)}\delta_{(i)} \end{bmatrix} + r_i \times F_i \quad j = 1, ..., n$$

$$0 \leq \omega_i \leq 10000$$

$$|\beta_i| \leq \pi/2$$

$$|\alpha_i| \leq \pi/6$$

Two algorithms are tested to perform the optimization problem, Genetic Algorithm and interior-point algorithm. These are implemented using MATLAB functions *ga* and *fmincon*. Two algorithms were developed for each method, an offline and a recursive algorithms. The objective of the recursive algorithm is to minimize the time for optimization to converge by optimizing for one sample with 12 inputs only at a time instead of optimizing for the 12 inputs in the whole flight samples

In Genetic Algorithm, the recursive technique is developed by setting the final population in one time sample to be the initial population in the next time sample. While in interior point optimization, the recursive algorithm is developed by setting the final solution at one time sample to be the initial set point in the next sample. Those techniques work only if the sampling time is small enough so that

there's no big difference between two consecutive samples.

4.4 Results

An initial comparison is carried out to choose which algorithm would be more suitable. The criteria for comparison are convergence time and optimality in terms of cost function. However, the first priority here is time for practical implementation purposes. The four algorithms are tested for 1, 2 and 3 samples of a flight simulation. The results are in table 4.4.

Samples		**GA**	**RGA**	**IP**	**RIP**
1	**conv. time**	898.0 s	898.0 s	0.6 s	0.6 s
	J	1.20	1.20	0.27	0.27
2	**conv. time**	12947.9 s	5357.4 s	2.4 s	1.3 s
	J	59.80	1.55	0.55	2.43
3	**conv. time**	38979.0 s	10497.4 s	13.9 s	2.0 s
	J	44.94	2.16	0.82	2.70

Table 4.1: Convergence Time and Objective Function Comparison

It's evident from the results that Recursive Interior-Point technique is more practical for our purpose. Although conventional IP technique is superior in optimality, which is expected, RIP takes significantly less time to converge which makes it the best candidate for online implementation. Further study is carried out on the developed RIP to investigate its behavior in terms of convergence time. Fig 4.2 shows the convergence time against number of samples optimized. The curve is almost linear except near the first few samples as shown in Fig. 4.3. The

slope of the linear part is equal to 0.270 m/sample. This means that the algorithm takes around 270 ms to optimize one sample of 12 inputs. This result is not suitable for online implementation, therefore all flight simulations are implemented offline. However, this result is very promising for future research.

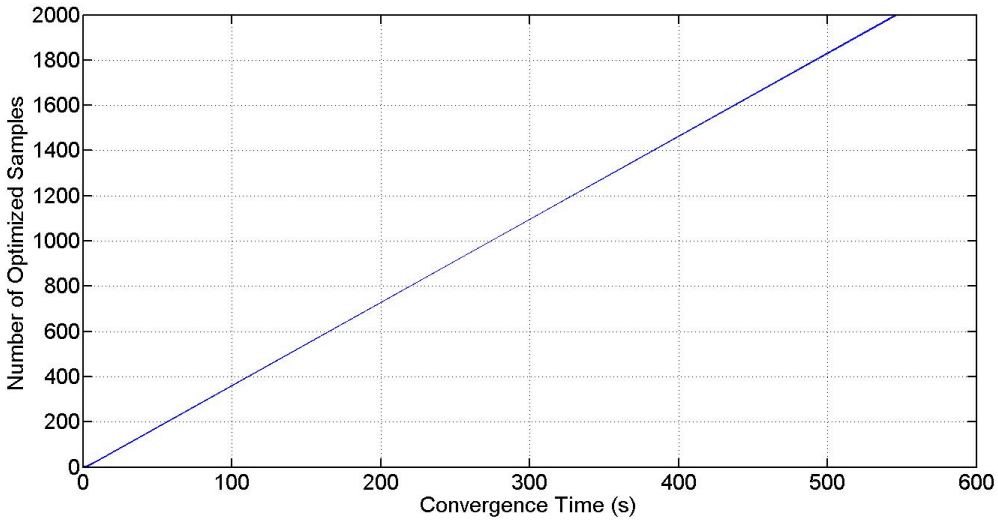

Figure 4.2: Convergence Time for Recursive Interior-Point Algorithm

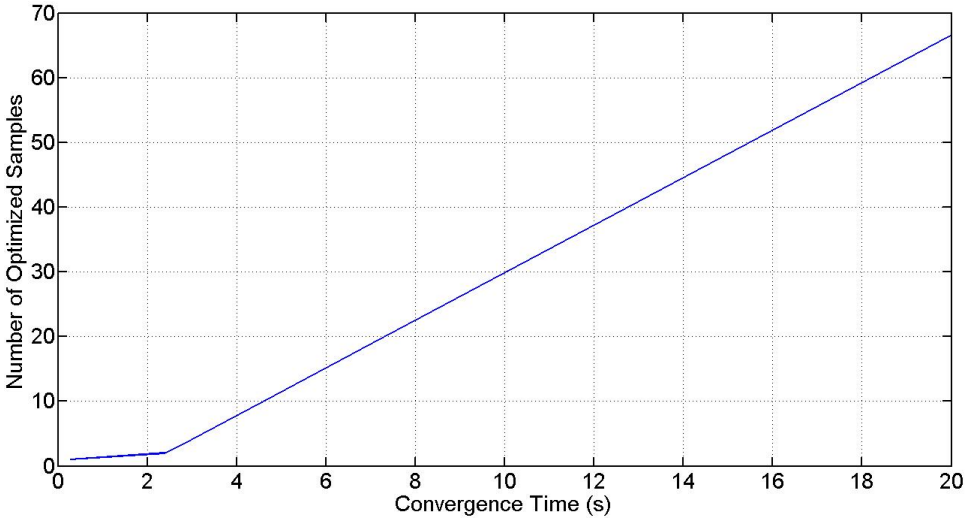

Figure 4.3: Convergence Time for Recursive Interior-Point Algorithm for Small Time

To test the control algorithm, the quadrotor is commanded to elevate up to $10m$, tilt forward with 30 degrees and perform a circle while pointing to its center. The flight is an example of a surveillance mission where the quadrotor might be taking panoramic photos of a certain target. This complex flight demonstrate the strength of both the design and control technique as five of the six states are commanded to perform completely independent but integrated tasks. The optimization is done offline, i.e, prior to the flight. The parameters of the system are assumed to be known and the control parameters are chosen according to *Theorem 1.* $K_{pF} = K_{pF} = I$ while $K_{vF} = K_{vM}$ are taken to be equal to $3I$, where I here is the $3x3$ identity matrix . To perform a circle, the quadrotor is commanded to follow sinusoidal paths along x and y axes. Figure 4.5 shows both the desired and actual positions of the quadrotor in x, y and z axes while figure 4.6

shows the first derivative of the position vector while the 3-D position is showed in figure 4.4. It's evident from the figures that the path was followed with high accuracy.

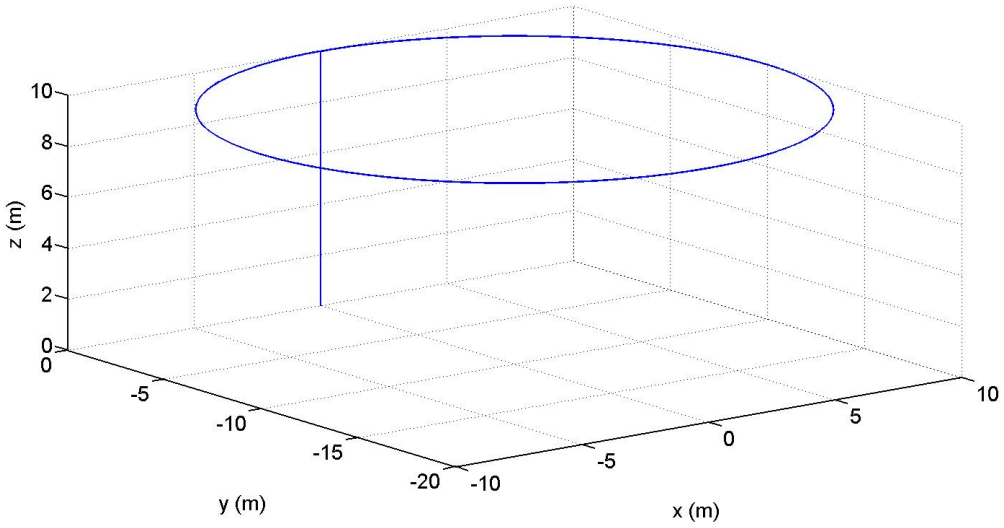

Figure 4.4: A 3D plot of the flight on x, y and z axes

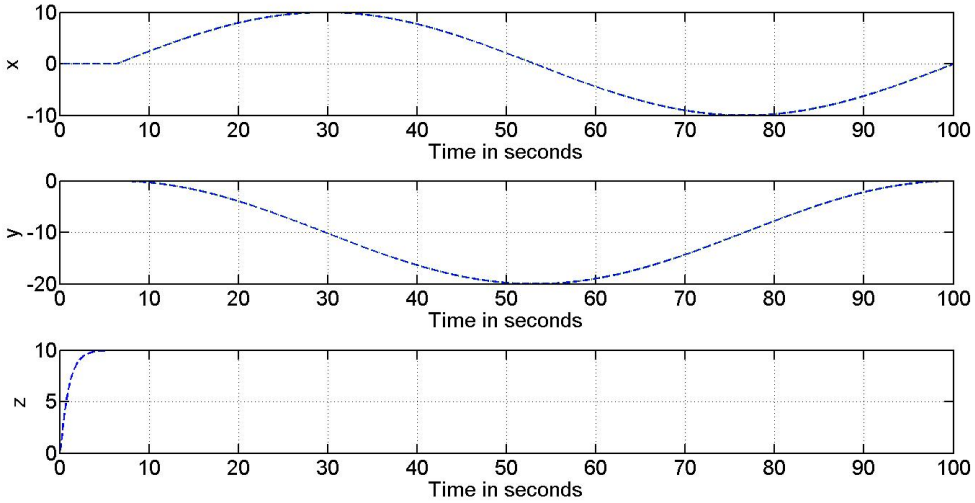

Figure 4.5: x, y and z positions of the quadrotor

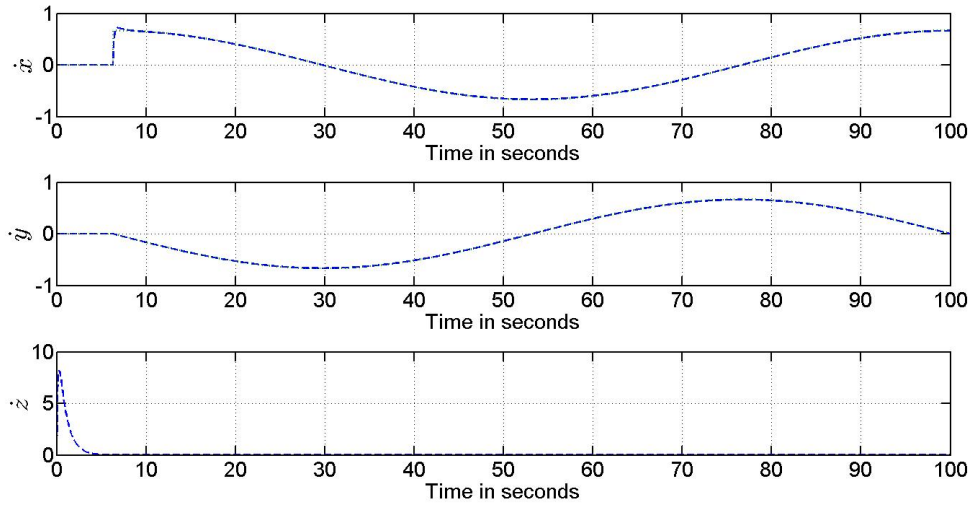

Figure 4.6: Translational velocities $\dot{x}$, $\dot{y}$ and $\dot{z}$

The orientation vector of the quadrotor is shown in figure 4.7 in radians. It can be seen that the angle Φ reached $\Pi/6$ and the angle Ψ went from 0 to 2Π to keep pointing towards the center of the circle while the quadrotor is completing a full circle. This means that Yaw angle is also performing a complete circle simultaneously.

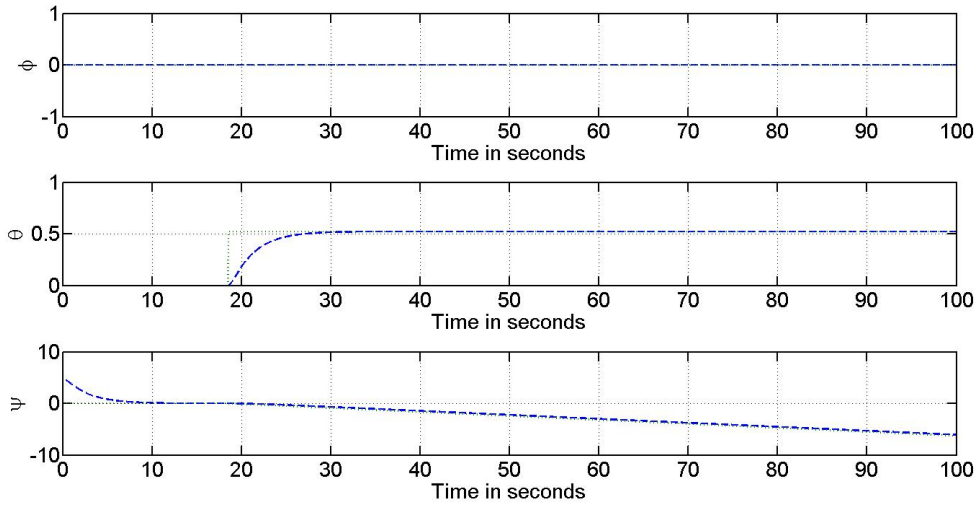

Figure 4.7: Quadrotor orientations Φ, Θ and Ψ

In Figure 4.8 and 4.9, the input angles α_i and β_i generated by optimization are shown. One objective of optimization was to limit the change in each of the angles in order to minimize energy consumption. The figures show very minimal variations in the angles. Figures 4.10 and 4.11 show the resulting forces and moments.

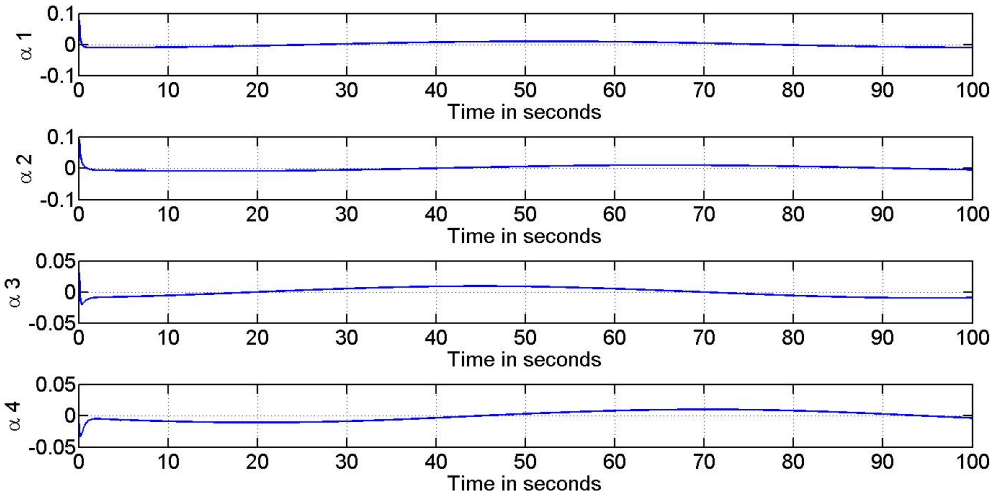

Figure 4.8: α_i generated by optimization

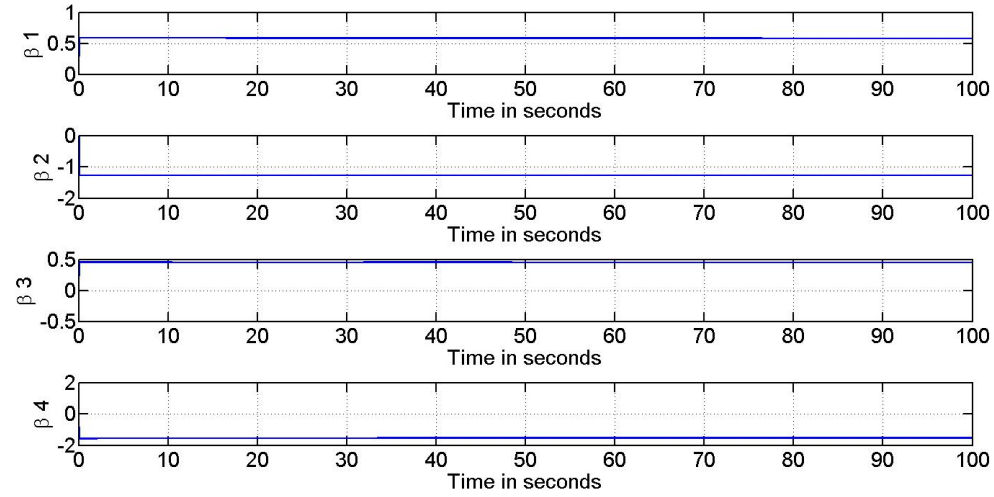

Figure 4.9: β_i generated by optimization

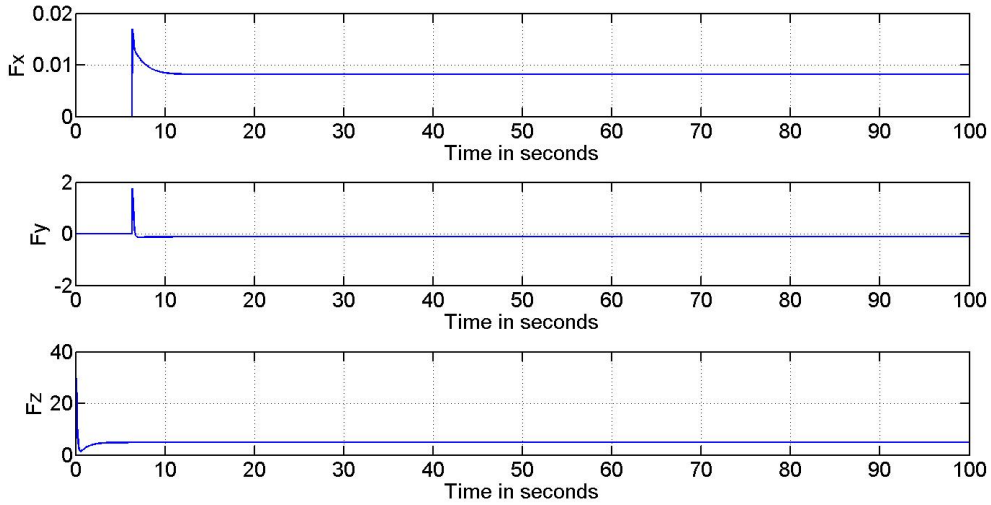

Figure 4.10: Desired forces generated by the controller

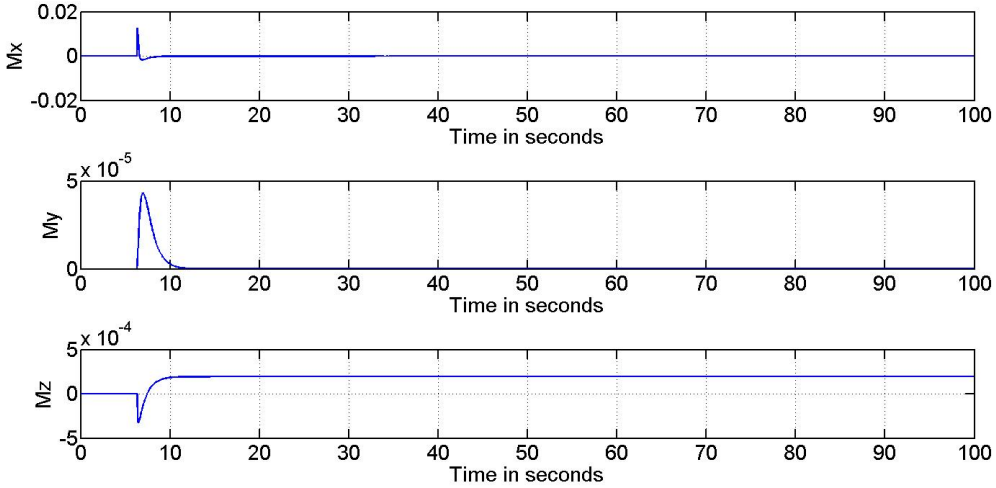

Figure 4.11: Desired moments generated by the controller

4.5 Conclusion

Feedback linearization proved to stabilized and control the attitude of the quadrotor. All the degrees of freedom can be controlled freely and independently. This allows for more complex and precise maneuvers that weren't possible with conventional quadrotor. In summary, this control algorithm highlights the advantages of the novel design by taking advantage of the high mechanical flexibility available. In fact, the controller decouples the model of the quadrotor into two completely separate systems, a systems of forces and positions, and a system of moments and orientations. The two systems can be studied and controlled absolutely independently. The only connection between the two systems appears in the final stage of optimization where the six equations are solved together to find the 12 inputs. The optimization part is developed to choose the best inputs according to energy consumption which is very critical in all UAV applications.

To sum up, the control and optimization part show very promising results. However, there is still a substantial space for improvements. Future research may include a wide variety of angles. Considering different scenarios of uncertainty in the parameters, states and disturbance. Optimization part as well can be further improved to consider different techniques and online implementation of optimization. Other control techniques can also be developed for this system. Particularly, model predictive control MPC is a candidate due to the fact that it combines control and optimization under constraints.

CHAPTER 5

CONCLUSION

In this work, a novel quadrotor design is introduced. The proposed design tackles the disadvantages of coupling and low fault tolerance capabilities which are present in conventional designs by allowing each rotor to tilt with two degree of freedom about a fixed frame which increases the number of inputs to 12 instead of 4. This addition aims to decouple all the motions of the system and improve fault tolerance capabilities. A mathematical model was developed for the proposed design and it was shown that the system is fully functional and the motions are completely decoupled with only two opposite rotors running. Initial simulation tests were carried out that prove the claimed advantages over conventional quadrotors.

To control the proposed quadrotor, a feedback linearization controller was developed and introduced through the forces and moments of the system as control inputs. The a way the controller was design aims to break the system down into two completely separate subsystems that can be controlled independently. The forces and moments are related to the actual 12 inputs of the system through

6 highly nonlinear equations. Offline optimization is introduced to solve the 6 equations and find the 12 input variables to achieve the desired forces and moments required by the controller with minimum energy. Stability analysis is studied for the controller using Lyaponove theory under different scenarios. The control algorithm with tested through simulation along with optimization and the results highlight the strength of this approach.

REFERENCES

[1] C. B. Fay, "A cursory analysis of the vtol tilt-wing performance and control problems," *Annals of the New York Academy of Sciences*, vol. 107, no. 1, pp. 102–146, Mar. 1963.

[2] K. Kondak, M. Bernard, N. Meyer, and G. Hommel, "Autonomously flying VTOL-robots: Modeling and control," in *2007 IEEE International Conference on Robotics and Automation*, Apr. 2007, pp. 736–741.

[3] D. Gurdan, J. Stumpf, M. Achtelik, K.-M. Doth, G. Hirzinger, and D. Rus, "Energy-efficient autonomous four-rotor flying robot controlled at 1 kHz," in *Robotics and Automation, 2007 IEEE International Conference on.* IEEE, 2007, pp. 361–366.

[4] J. Kim, M.-S. Kang, and S. Park, "Accurate modeling and robust hovering control for a quad-rotor VTOL aircraft," in *Selected papers from the 2nd International Symposium on UAVs, Reno, Nevada, U.S.A. June 10, 2009*, K. P. Valavanis, R. Beard, P. Oh, A. Ollero, L. A. Piegl, and H. Shim, Eds. Springer Netherlands, Jan. 2010, pp. 9–26.

[5] S. Grzonka, G. Grisetti, and W. Burgard, "A fully autonomous indoor quadrotor," *Robotics, IEEE Transactions on*, vol. 28, no. 1, pp. 90–100, 2012.

[6] E. Capello, A. Scola, G. Guglieri, and F. Quagliotti, "Mini quadrotor UAV: design and experiment," *Journal of Aerospace Engineering*, vol. 25, no. 4, pp. 559–573, 2012.

[7] P. Pounds, R. Mahony, and P. Corke, "Modelling and control of a large quadrotor robot," *Control Engineering Practice*, vol. 18, no. 7, pp. 691–699, 2010.

[8] A. Tayebi and S. McGilvray, "Attitude stabilization of a VTOL quadrotor aircraft," *IEEE Transactions on Control Systems Technology*, vol. 14, no. 3, pp. 562–571, May 2006.

[9] M. Rich, "Model development, system identification, and control of a quadrotor helicopter," 2012.

[10] P. Pounds, R. Mahony, P. Hynes, and J. Roberts, "Design of a four-rotor aerial robot," in *Australasian Conference on Robotics and Automation*, 2002, pp. 145–150.

[11] Y. Naidoo, R. Stopforth, and G. Bright, "Quad-rotor unmanned aerial vehicle helicopter modelling & control," *Int J Adv Robotic Sy*, vol. 8, no. 4, pp. 139–149, 2011.

[12] P. C. Garcia, R. Lozano, and A. E. Dzul, *Modelling and Control of Mini-Flying Machines*. Springer Science & Business Media, Mar. 2006.

[13] B. Herisse, F.-X. Russotto, T. Hamel, and R. Mahony, "Hovering flight and vertical landing control of a VTOL unmanned aerial vehicle using optical flow," in *IEEE/RSJ International Conference on Intelligent Robots and Systems, 2008. IROS 2008*, Sep. 2008, pp. 801–806.

[14] "Dynamic model and control of a new quadrotor unmanned aerial vehicle with tilt-wing mechanism."

[15] A. Sanchez, J. Escareno, O. Garcia, R. Lozano, and others, "Autonomous hovering of a noncyclic tiltrotor UAV: Modeling, control and implementation," in *Proc. of the 17th IFAC Wold Congress*, 2008, pp. 803–808.

[16] F. Kendoul, I. Fantoni, and R. Lozano, "Modeling and control of a small autonomous aircraft having two tilting rotors," in *Decision and Control, 2005 and 2005 European Control Conference. CDC-ECC'05. 44th IEEE Conference on.* IEEE, 2005, pp. 8144–8149.

[17] S. K. Phang, C. Cai, B. M. Chen, and T. H. Lee, "Design and mathematical modeling of a 4-standard-propeller (4sp) quadrotor," in *Intelligent Control and Automation (WCICA), 2012 10th World Congress on.* IEEE, 2012, pp. 3270–3275.

[18] M. Ryll, H. H. Bulthoff, and P. R. Giordano, "Modeling and control of a quadrotor UAV with tilting propellers," in *Robotics and Automation (ICRA), 2012 IEEE International Conference on.* IEEE, 2012, pp. 4606–4613.

[19] A. Krings, "Fault tolerant system design," *JEB*, vol. 320, no. 208, pp. 885–4078, 2011.

[20] R. J. Patton, "Fault-tolerant control systems: The 1997 situation," in *IFAC symposium on fault detection supervision and safety for technical processes*, vol. 3, 1997, pp. 1033–1054.

[21] A. Freddi, A. Lanzon, and S. Longhi, "A feedback linearization approach to fault tolerance in quadrotor vehicles," in *Proceedings of The 2011 IFAC World Congress, Milan, Italy*, 2011.

[22] F. Sharifi, M. Mirzaei, B. W. Gordon, and Y. Zhang, "Fault tolerant control of a quadrotor UAV using sliding mode control," in *Control and Fault-Tolerant Systems (SysTol), 2010 Conference on*. IEEE, 2010, pp. 239–244.

[23] H. Alwi, M. T. Hamayun, and C. Edwards, "An integral sliding mode fault tolerant control scheme for an octorotor using fixed control allocation," in *Variable Structure Systems (VSS), 2014 13th International Workshop on*. IEEE, 2014, pp. 1–6.

[24] H. Alwi and C. Edwards, "LPV sliding mode fault tolerant control of an octorotor using fixed control allocation," in *Control and Fault-Tolerant Systems (SysTol), 2013 Conference on*. IEEE, 2013, pp. 772–777.

[25] R. W. Brockett, "Feedback invariants for nonlinear systems," 1979.

[26] B. Charlet, J. Lvine, and R. Marino, "On dynamic feedback linearization," *Systems & Control Letters*, vol. 13, no. 2, pp. 143–151, 1989.

[27] R. B. Gardner and W. F. Shadwick, "Symmetry and the implementation of feedback linearization," *Systems & Control Letters*, vol. 15, no. 1, pp. 25–33, Jul. 1990.

[28] W. Shadwick and W. Sluis, "Dynamic feedback linearization," in *, Proceedings of the 29th IEEE Conference on Decision and Control, 1990*, Dec. 1990, pp. 2085–2087 vol.4.

[29] W. F. Shadwick, "Absolute equivalence and dynamic feedback linearization," *Systems & Control Letters*, vol. 15, no. 1, pp. 35–39, Jul. 1990.

[30] E. Aranda-Bricaire, C. Moog, and J.-B. Pomet, "A linear algebraic framework for dynamic feedback linearization," *IEEE Transactions on Automatic Control*, vol. 40, no. 1, pp. 127–132, Jan. 1995.

[31] H. Voos, "Nonlinear control of a quadrotor micro-UAV using feedback-linearization," in *Mechatronics, 2009. ICM 2009. IEEE International Conference on.* IEEE, 2009, pp. 1–6.

[32] S. Al-Hiddabi, "Quadrotor control using feedback linearization with dynamic extension," in *Mechatronics and its Applications, 2009. ISMA'09. 6th International Symposium on.* IEEE, 2009, pp. 1–3.

[33] A. Benallegue, A. Mokhtari, and L. Fridman, "Feedback linearization and high order sliding mode observer for a quadrotor UAV," in *Variable Structure Systems, 2006. VSS'06. International Workshop on.* IEEE, 2006, pp. 365–372.

[34] D. Lee, H. J. Kim, and S. Sastry, "Feedback linearization vs. adaptive sliding mode control for a quadrotor helicopter," *International Journal of Control, Automation and Systems*, vol. 7, no. 3, pp. 419–428, 2009.

[35] J. Renegar, *A mathematical view of interior-point methods in convex optimization*. Siam, 2001, vol. 3.

[36] "An interior point algorithm for large-scale nonlinear optimization with applications in process engineering," Ph.D. dissertation.

[37] D. E. Goldberg, *Genetic Algorithms in Search, Optimization and Machine Learning*, 1st ed. Boston, MA, USA: Addison-Wesley Longman Publishing Co., Inc., 1989.

[38] A. Homaifar, C. X. Qi, and S. H. Lai, "Constrained optimization via genetic algorithms," *Simulation*, vol. 62, no. 4, pp. 242–253, 1994.

[39] C. M. Fonseca and P. J. Fleming, "An overview of evolutionary algorithms in multiobjective optimization," *Evolutionary computation*, vol. 3, no. 1, pp. 1–16, 1995.

[40] Z. Michalewicz, C. Z. Janikow, and J. B. Krawczyk, "A modified genetic algorithm for optimal control problems," *Computers & Mathematics with Applications*, vol. 23, no. 12, pp. 83–94, Jun. 1992.

[41] H. O. Fattorini, *Infinite Dimensional Optimization and Control Theory*. Cambridge University Press, Mar. 1999.

[42] M. V. Kothare, V. Balakrishnan, and M. Morari, "Robust constrained model predictive control using linear matrix inequalities," *Automatica*, vol. 32, no. 10, pp. 1361–1379, Oct. 1996.

[43] Z. Michalewicz and G. Nazhiyath, "Genocop III: A co-evolutionary algorithm for numerical optimization problems with nonlinear constraints," in *Evolutionary Computation, 1995., IEEE International Conference on*, vol. 2. IEEE, 1995, pp. 647–651.

[44] S. Wang and X. Jin, "Model-based optimal control of VAV air-conditioning system using genetic algorithm," *Building and Environment*, vol. 35, no. 6, pp. 471–487, Aug. 2000.

Vitae

- Name: Mahmoud Elfeky
- Nationality: Egypt
- Date of Birth: 01-01-1989
- Email: *Fq.mahmoud@gmail.com*